Heparan sulfate proteoglycan syndecan-3 is a novel receptor for GDNF, neurturin, and artemin

Maxim M. Bespalov,[1] Yulia A. Sidorova,[1] Sarka Tumova,[2] Anni Ahonen-Bishopp,[2] Ana Cathia Magalhães,[1] Evgeny Kulesskiy,[2] Mikhail Paveliev,[1] Claudio Rivera,[1] Heikki Rauvala,[2] and Mart Saarma[1]

[1]Institute of Biotechnology, Viikki Biocenter, and [2]Neuroscience Center, University of Helsinki, Helsinki 00014, Finland

Glial cell line–derived neurotrophic factor (GDNF) family ligands (GFLs) are potent survival factors for dopaminergic neurons and motoneurons with therapeutic potential for Parkinson's disease. Soluble GFLs bind to a ligand-specific glycosylphosphatidylinositol-anchored coreceptor (GDNF family receptor α) and signal through the receptor tyrosine kinase RET. In this paper, we show that all immobilized matrix-bound GFLs, except persephin, use a fundamentally different receptor. They interact with syndecan-3, a transmembrane heparan sulfate (HS) proteoglycan, by binding to its HS chains with high affinity. GFL–syndecan-3 interaction mediates both cell spreading and neurite outgrowth with the involvement of Src kinase activation. GDNF promotes migration of cortical neurons in a syndecan-3–dependent manner, and in agreement, mice lacking syndecan-3 or GDNF have a reduced number of cortical γ-aminobutyric acid–releasing neurons, suggesting a central role for the two molecules in cortical development. Collectively, syndecan-3 may directly transduce GFL signals or serve as a coreceptor, presenting GFLs to the signaling receptor RET.

Introduction

Glial cell line–derived neurotrophic factor (GDNF), neurturin (NRTN), artemin (ARTN), and persephin (PSPN) are secreted growth factors collectively known as GDNF family ligands (GFLs). GFLs play a pivotal role in differentiation and maintenance of the nervous system and, in the case of GDNF, in kidney development and spermatogenesis (Bespalov and Saarma, 2007). GFLs have pharmaceutical potential for the treatment of neurological diseases. In particular, GDNF has shown very promising results in two Parkinson's disease clinical trials (Gill et al., 2003; Slevin et al., 2005), although a larger placebo-controlled study failed to show clear clinical benefits of GDNF (Lang et al., 2006). GDNF is also a potent survival factor for central motoneurons and may have a clinical potential in the treatment of amyotrophic lateral sclerosis (Henderson et al., 1994).

The conventional receptor complex for soluble GFLs consists of a ligand-specific glycosylphosphatidylinositol (GPI)-anchored coreceptor, GDNF family receptor α (GFR-α), and a signal-transducing module, the receptor tyrosine kinase RET, or, in some cells, neural cell adhesion molecule (NCAM; Paratcha et al., 2003). GDNF activates either RET or NCAM via GFR-α1, NRTN via GFR-α2, ARTN via GFR-α3, and PSPN uses GFR-α4. Notably, GDNF promotes differentiation and tangential migration of embryonic cortical γ-aminobutyric acid (GABA)–releasing (GABAergic) neurons that lack both RET and NCAM (Pozas and Ibáñez, 2005). An unknown receptor may thus mediate some GDNF-dependent processes in cortical development.

Growth factor signaling is critically modulated by the ECM. The activities of many growth factors are affected by

Correspondence to Mart Saarma: Mart.Saarma@helsinki.fi

M. Paveliev's current address is Neuroscience Center, University of Helsinki, Helsinki 00014, Finland.

S. Tumova's current address is Institute of Membrane and Systems Biology, Faculty of Biological Sciences, University of Leeds, Leeds LS2 9JT, England, UK.

A. Ahonen-Bishopp's current address is Biocomputing Platforms Ltd., Espoo 002150, Finland.

Abbreviations used in this paper: ARTN, artemin; BDNF, brain-derived neurotrophic factor; FRET, Förster resonance energy transfer; GABA, γ-aminobutyric acid; GDNF, glial cell line–derived neurotrophic factor; GE, ganglionic eminence; GFL, GDNF family ligand; GFR-α, GDNF family receptor α; GPI, glycosylphosphatidylinositol; HB-GAM, heparin-binding growth-associated molecule; HS, heparan sulfate; HSPG, HS proteoglycan; IZ, intermediate zone; MGE, medial GE; NCAM, neural cell adhesion molecule; NRTN, neurturin; PI-PLC, phosphatidylinositol-specific PLC; PSPN, persephin; SFK, Src family kinase; SPR, surface plasmon resonance; wtGDNF, wild-type GDNF.

Supplemental material can be found at:
http://doi.org/10.1083/jcb.201009136

The Rockefeller University Press $30.00
J. Cell Biol.
www.jcb.org/cgi/doi/10.1083/jcb.201009136

interaction with ECM heparan sulfates (HSs) presented by HS proteoglycans (HSPGs). In addition, cell surface HSPGs, in particular syndecans, act as coreceptors for many growth factors and adhesion molecules (Bernfield et al., 1999; Bishop et al., 2007). A member of the family, syndecan-3 (neuronal syndecan or N-syndecan), is a signal-transducing receptor for ECM-located heparin-binding growth-associated molecule (HB-GAM; also known as pleiotrophin; Raulo et al., 1994; Kinnunen et al., 1998). HB-GAM binding to HS chains of syndecan-3 activates Src family kinases (SFKs), leading to hippocampal neurite outgrowth and neuronal migration (Kinnunen et al., 1998; Rauvala et al., 2000; Hienola et al., 2006). Interestingly, only immobilized HB-GAM can trigger this biological response via syndecan-3, whereas free (soluble) HB-GAM acts as an inhibitor (Raulo et al., 1994; Kinnunen et al., 1998).

GDNF was originally purified by heparin affinity chromatography (Lin et al., 1993) and has later been shown to interact with HS (Rickard et al., 2003). HSs are required for GDNF signaling through the GFR-α1–RET complex (Barnett et al., 2002; Parkash et al., 2008). Recently, ARTN and NRTN interaction with heparin was demonstrated (Silvian et al., 2006; Alfano et al., 2007). Almost nothing is known about the interaction of PSPN with heparin, and the molecular identity of HSPGs that bind GFLs has remained obscure.

In the present study, we elucidate heparin and HS binding to the individual members of the GFL family. We find that syndecan-3 acts as a functional receptor for immobilized GDNF, triggering cell spreading and neurite outgrowth via SFK activation. Our migration assays implicate GDNF–syndecan-3 signaling in the regulation of brain cortex development. The results suggest a dual mode of action for GDNF, namely signaling via conventional receptors, such as RET or NCAM, in a free form, whereas immobilized matrix-bound GDNF would signal through syndecan-3.

Results

GDNF, NRTN, and ARTN interact with heparin and HSPG syndecan-3

We first asked whether all GFLs bind heparin and what structural determinants of heparin are required for this interaction. Putative heparin binding sites (Cardin and Weintraub, 1989; Hileman et al., 1998) are present in the primary structure of GDNF, NRTN, and ARTN but not in PSPN. In agreement, ^{125}I-labeled GDNF, NRTN, and ARTN bind to the heparin–Sepharose column (Fig. 1 A), whereas PSPN does not. The affinity of GFLs for heparin and HS was measured by surface plasmon resonance (SPR), implementing dynamics and an equilibrium response. The dissociation constants (K_ds) for GDNF, NRTN, and ARTN were all between 10 and 50 nM, with the exception of the dynamics-derived K_d for NRTN, which was >100 nM. PSPN had three orders of magnitude lower affinity for heparin than the other ligands; the K_d was 29.1 µM (dynamics) or 11.1 µM (equilibrium; Table S1 and Fig. 1 B). The affinity of ^{3}H-labeled heparin for GDNF was confirmed using a third independent method, scintillation proximity assay (Leppänen et al., 2004), yielding a similar K_d (~10 nM; unpublished data).

Structural specificity of the heparin–GDNF interaction was studied by SPR using desulfated heparins. Specific removal of 2-*O*-sulfate, 6-*O*-sulfate, and *N*-sulfate groups from heparin significantly impaired the interaction with GDNF, as determined by both competition assays with heparin and direct binding to GDNF (Fig. S1). Our results support the earlier observation that 2-O-sulfation is crucial for GDNF interaction with heparin (Rickard et al., 2003; Rider, 2003), although in our assays, 6-O- and N-sulfation were also important.

To test whether heparin-binding GFLs would bind to natural HSPGs, we used SPR to assay the direct interaction between immobilized GFLs and the HS-carrying extracellular domain of syndecan-3 purified from rat brain (Raulo et al., 1994). The K_ds for GDNF, NRTN, and ARTN were in the 10–50-nM range (Fig. 2 A), indicating high affinity binding to syndecan-3 and supporting the notion that these GFLs could directly interact with HSPGs at the cell surface and/or in the ECM. The binding occurs specifically via HS chains because heparinase III treatment strongly inhibited the interaction of GDNF and syndecan-3 (Fig. 2 B). For PSPN dynamics, data could not be fit with a simple curve, and because of limiting concentrations of syndecan-3, K_d was only estimated to be >70 nM. Thus, it appears that PSPN binds syndecan-3 with much lower affinity than the rest of the GFLs (Fig. 2 A).

The interaction between GDNF and syndecan-3 in a cellular context was studied by chemical cross-linking and by Förster resonance energy transfer (FRET). Chemical cross-linking of ^{125}I-GDNF to C6 cells, a rat glioma cell line, which expresses syndecan-3 (Kinnunen et al., 1998), followed by immunoprecipitation with syndecan-3 antibodies revealed a specific interaction of GDNF and syndecan-3 on the cell surface (Fig. 2 B). A high molecular weight complex visualized by autoradiography represents the GDNF complex with a syndecan-3 oligomer. The interaction was displaced by an excess of unlabeled (cold) GDNF or HB-GAM, another syndecan-3–specific ligand. Addition of 1 µg/ml heparin or removing HS chains by heparinase III treatment abolished ^{125}I-GDNF binding to syndecan-3 almost completely (Fig. 2 B), confirming the involvement of HS chains in the interaction. To exclude the possibility of GPI-anchored GFR-α1 involvement in the GDNF interaction with syndecan-3 on the cell surface, we treated C6 cells with phosphatidylinositol-specific PLC (PI-PLC). This treatment had no significant effect on ^{125}I-GDNF binding to syndecan-3, indicating that GFR-α1 is not required for the GDNF–syndecan-3 complex formation. In addition, the data on PI-PLC treatment indicate that the cell surface GPI-linked HSPGs, glypicans, are not involved in the interaction.

To study the effects of GDNF on syndecan-3 localization, human embryonic kidney cells were transiently transfected with syndecan-3, which was C-terminally fused with CFP or YFP (Hienola et al., 2006). GDNF induced a rapid syndecan-3 oligomerization on the plasma membrane, as determined from an increase in FRET between the two fluorophores (Fig. 2 D). Collectively, these results allowed us to conclude that GDNF, ARTN, and NRTN, but not PSPN, bind heparin and syndecan-3 with high affinity and that interaction between GDNF and HS chains of syndecan-3 on the cell surface triggers the proteoglycan oligomerization.

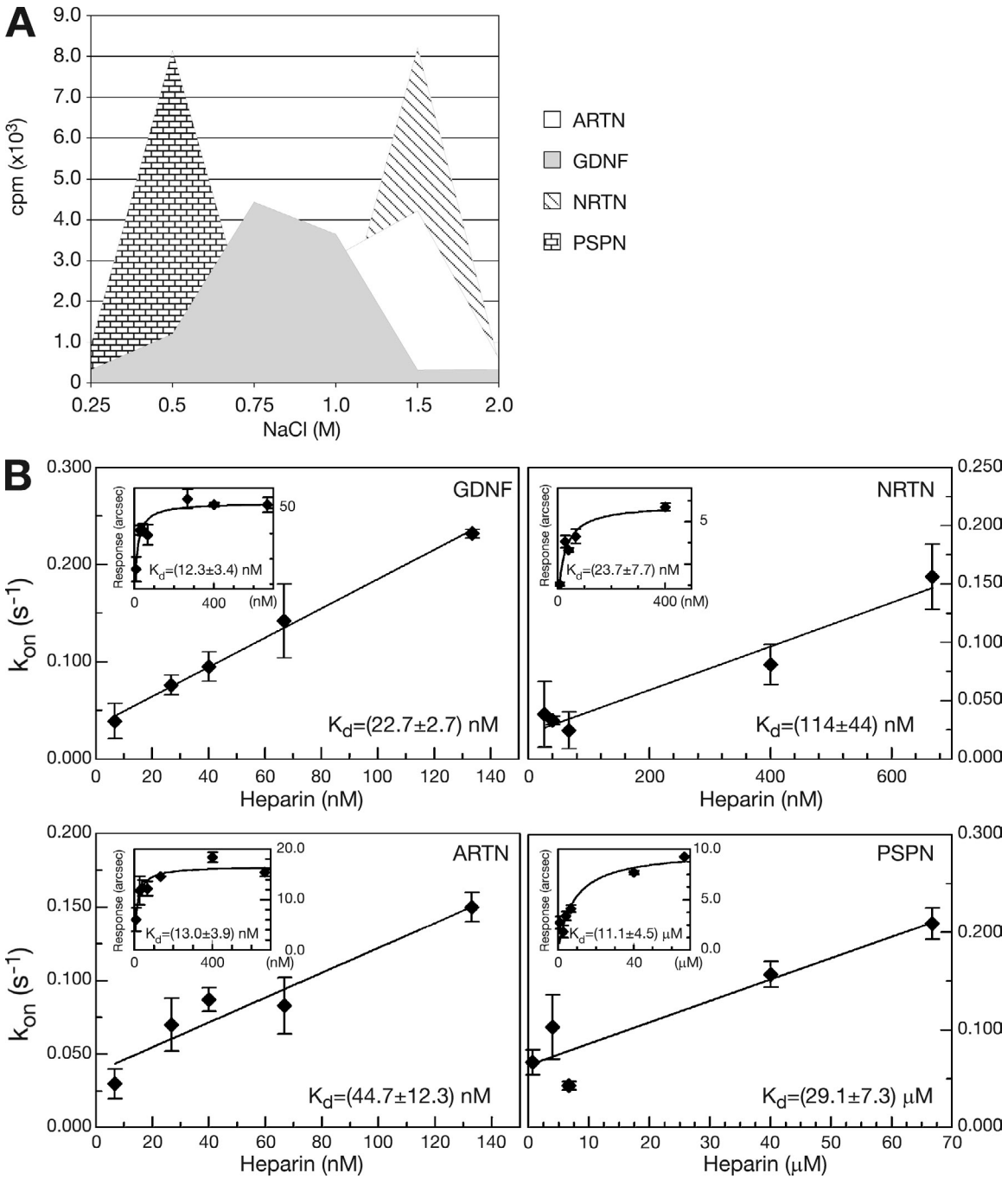

Figure 1. **GFL binding to heparin.** (A) Elution of ^{125}I-GFLs from a heparin–Sepharose column by a step-wise NaCl gradient. PSPN elutes at a 0.5-M NaCl concentration, indicating a very weak interaction with heparin. GDNF elutes from the heparin column at a 0.75–1-M NaCl concentration, ARTN elutes at a 1–1.5-M NaCl concentration, and NRTN elutes at a 1.5-M NaCl concentration. (B) Heparin binding to immobilized GFLs was followed by SPR using the IAsys optical biosensor. The K_ds were determined from dynamics as well as equilibrium data (insets), and their values are indicated in the graphs. Error bars show SEM from three to four experiments for each condition. K_{on} is the association rate constant. arcsec, arcsecond.

GDNF localization in the ECM and GFL-induced cell spreading

Immobilized and diffusible molecules differentially regulate neuronal development and maintenance. It is generally thought that most neurotrophic factors, including GFLs, act as diffusible soluble proteins. In contrast, the ECM molecule HB-GAM signals through syndecan-3 only as an immobilized matrix-bound protein and is not active as a soluble (diffusible) protein at physiological concentrations (Raulo et al., 1994; Kinnunen et al., 1998). Intriguingly, the ability of GFLs to interact with HSPGs raises the question of whether GFLs are bound to ECM in the tissue and, if so, whether this affects their biological activity.

To answer the first question, we used juvenile kidney and brain, in which GDNF is relatively abundant and can be readily detected. We performed biochemical fractionation of juvenile mice tissues followed by Western blotting. We found GDNF in the ECM fraction of the postnatal brain and kidney (Fig. 2 C). Lower amounts of GDNF were associated with the

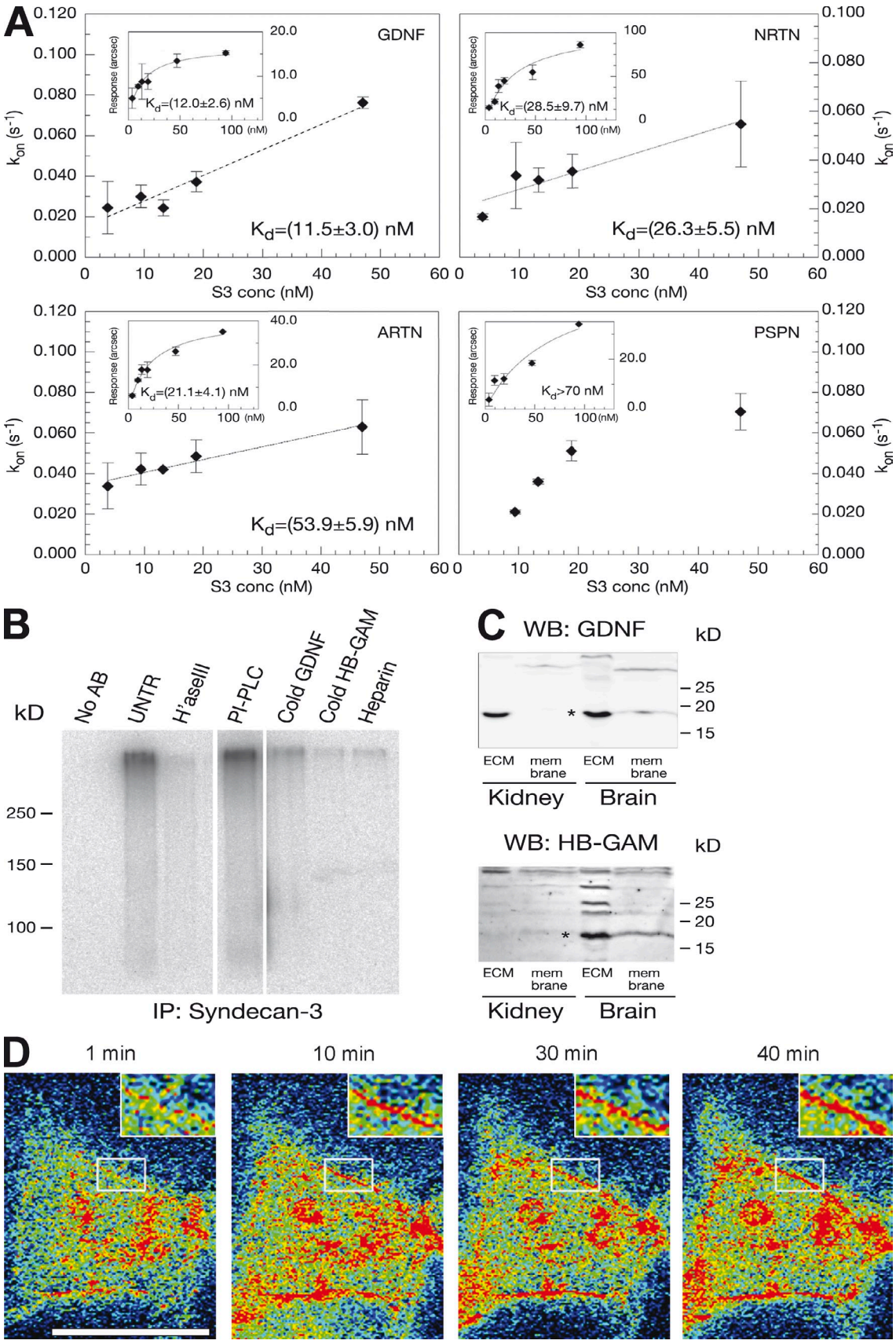

Figure 2. **GDNF, NRTN, and ARTN bind directly to syndecan-3 with high affinity.** (A) Syndecan-3 (S3) binding to GFLs, immobilized on the cuvette, was followed by SPR. The K_ds were determined from dynamics as well as equilibrium data (insets), and their values are indicated in the graphs. Error bars show SEM from three to four experiments for each condition. K_{on} is the association rate. arcsec, arcsecond. conc, concentration. (B) GDNF interacts directly with

plasma membrane. HB-GAM was used as a marker for the brain ECM.

To test the biological effects of immobilized GFLs, we took advantage of the human neuroblastoma cell line SHEP, which lacks RET (as determined by PCR with specific human RET primers) but expresses the GDNF coreceptor GFR-α1 (Poteryaev et al., 1999). SHEP cells also express syndecan-3 (Fig. 3 A). Immobilized on plastic microplates, GDNF, NRTN, and ARTN, but not PSPN, induced adherence and spreading of SHEP cells (Fig. 3, B and C). Spreading on immobilized GFLs involved 60–80% of the cells (Fig. 3, B and C) and occurred within 10–20 min after settling (Video 1). The spreading was accompanied by actin rearrangement and stress fiber formation (unpublished data), suggesting GFL-induced signaling.

For successful spreading of SHEP cells on immobilized GFLs, HSPGs are required because heparinase III treatment almost completely abolished cell attachment and spreading (Fig. 3, B and C). Heparinase III had no effect on SHEP cell adhesion and spreading on uncoated tissue culture plates (Fig. 3 C), indicating that the cellular machinery responsible for the observed adhesion was not affected and that the enzyme specifically disrupts the HS–GFL interactions. In agreement, SHEP cells failed to adhere and spread on PSPN or BSA, which lack affinity for HS. Treatment of SHEP cells with PI-PLC, an enzyme that cleaves the GPI anchor (Fig. 3 D), did not affect their attachment and spreading on GFL-coated surfaces despite blocking soluble GDNF signaling via GFR-α1 (not depicted). These results suggest a GFR-α1–independent mechanism for immobilized GFL signaling.

To further evaluate the role of GFR-α1 and RET in immobilized GDNF-induced cell spreading, we preincubated the GDNF-coated plate and the SHEP cells with GDNF function-blocking antibodies. These antibodies prevent GDNF binding to GFR-α1–RET but do not affect GDNF interaction with HS of syndecan-3 as they block the central part of GDNF (Xu et al., 1998), which is dispensable for interaction with HS. Neither this treatment nor NCAM function-blocking antibodies had any effect on attachment and spreading of SHEP cells induced by immobilized GDNF (Fig. 3 D). Adherence of SHEP cells to GDNF is also independent of another polysaccharide related to HS. Chondroitin sulfate proteoglycans are not involved in the adhesion because it was not affected by removal of chondroitin sulfate chains from the cell surface by chondroitin sulfate lyase ABC (Fig. 3 D). Because SHEP cells do not express RET, we conclude that their attachment and spreading on immobilized GDNF, ARTN, or NRTN is a RET-independent process.

To further confirm the involvement of HSPG, we generated a GDNF mutant that lacks 38 N-terminal amino acids (ΔN-GDNF) and does not bind to heparin (Fig. S2 C; Alfano et al., 2007). The N-terminal deletion does not significantly affect the ability of soluble ΔN-GDNF to activate the conventional GFR-α1–RET receptor complex but may have weaker affinity to GFR-α1 when expressed in the absence of RET (Fig. S2 A; Eketjäll et al., 1999). Soluble ΔN-GDNF mutant was also shown to be biologically active (Fig. S2 B) in previously reported GFR-α–RET-mediated neurite outgrowth assays on dorsal root ganglia neurons (Paveliev et al., 2004). This GDNF variant also stimulates MAPK signaling and promotes survival of dopaminergic neurons in vivo (Piltonen et al., 2009). However, immobilized ΔN-GDNF failed to induce attachment and spreading of SHEP cells (Fig. 3 D), indicating a requirement for HS interaction with immobilized GDNF. These results suggest that GDNF has two modes of action: as a diffusible free protein activating GFR-α1–RET receptors and as an immobilized matrix-bound protein activating the signaling complex based on HSPG. Thus, HSPGs may serve as coreceptors for GFLs and/or deliver the growth factors to GFR-α1 or NCAM receptors.

GDNF interaction with HSPGs is required for Src kinase activation

Immobilized GDNF induces activation of SFKs in SHEP cells that is HSPG dependent, as it is abolished by heparinase III treatment and does not occur on ΔN-GDNF (Fig. 3 E). In addition, SFK activation may not depend on GFR-α1, as suggested by the lack of signaling inhibition by PI-PLC treatment (Fig. 3 E). Pretreatment of SHEP cells with the selective and nontoxic SFK inhibitor SU6656 (Paveliev et al., 2004) diminished their spreading on immobilized GDNF (Fig. 3 F) but did not impair their adherence. Similar results were obtained with cells infected with a dominant-negative Src kinase adenovirus (Fig. 3 G), suggesting that SFK activation is required for SHEP cell spreading but not for their attachment on immobilized GDNF. These results are compatible with the HB-GAM–induced syndecan-3 signaling that requires HS chains and regulates the cytoskeleton through the cortactin–SFK pathway (Rauvala et al., 2000).

Immobilized GDNF induces neurite outgrowth using HSPG

Cell spreading is a crucial step in many biological processes, including cell migration and neurite outgrowth. Soluble GFLs induce neurite outgrowth in a variety of neurons in vitro. To find out whether syndecan-3 interaction with immobilized GDNF is

syndecan-3 in the rat glioma C6 cell line. Chemical cross-linking of ^{125}I-GDNF to C6 cells was followed by immunoprecipitation (IP) with antisyndecan-3 antibodies in untreated cells (UNTR), cells pretreated with heparinase III (H'ase III), and cells pretreated with phosphatidylinositol-specific PLC (PI-PLC). Alternatively, a 150-fold molar excess of unlabeled (cold) GDNF and HB-GAM or 1 µg/ml heparin was added simultaneously with ^{125}I-GDNF. In the negative control, no syndecan-3 antibodies were added (No AB). The high molecular mass band in the top of the gel corresponds to the GDNF–syndecan-3 complex. Equal loading of the proteins was confirmed by silver staining of the gel (not depicted). (C) Western blotting (WB) of proteins extracted from dissociated P9 mouse brain and kidney tissues. Lysates from ECM and membrane-associated fractions were separated by SDS-PAGE, and Western blots were probed with anti-GDNF (top) or anti–HB-GAM antibodies (bottom). The bands corresponding to GDNF and HB-GAM are marked with asterisks. Molecular mass markers are shown on the right. (D) GDNF-induced syndecan-3 oligomerization visualized by FRET. FRET channel images of human embryonic kidney cells transiently transfected with syndecan-3 fusion constructs with YFP or CFP and stimulated with 100 ng/ml GDNF. Images were taken after GDNF stimulation at varying time points. FRET-corrected images were displayed in pseudocolors (red areas indicate high values of FRET, and blue areas indicate low values of FRET). Insets highlight a strong FRET signal at the plasma membrane, where syndecan-3 is targeted. Bar, 10 µM.

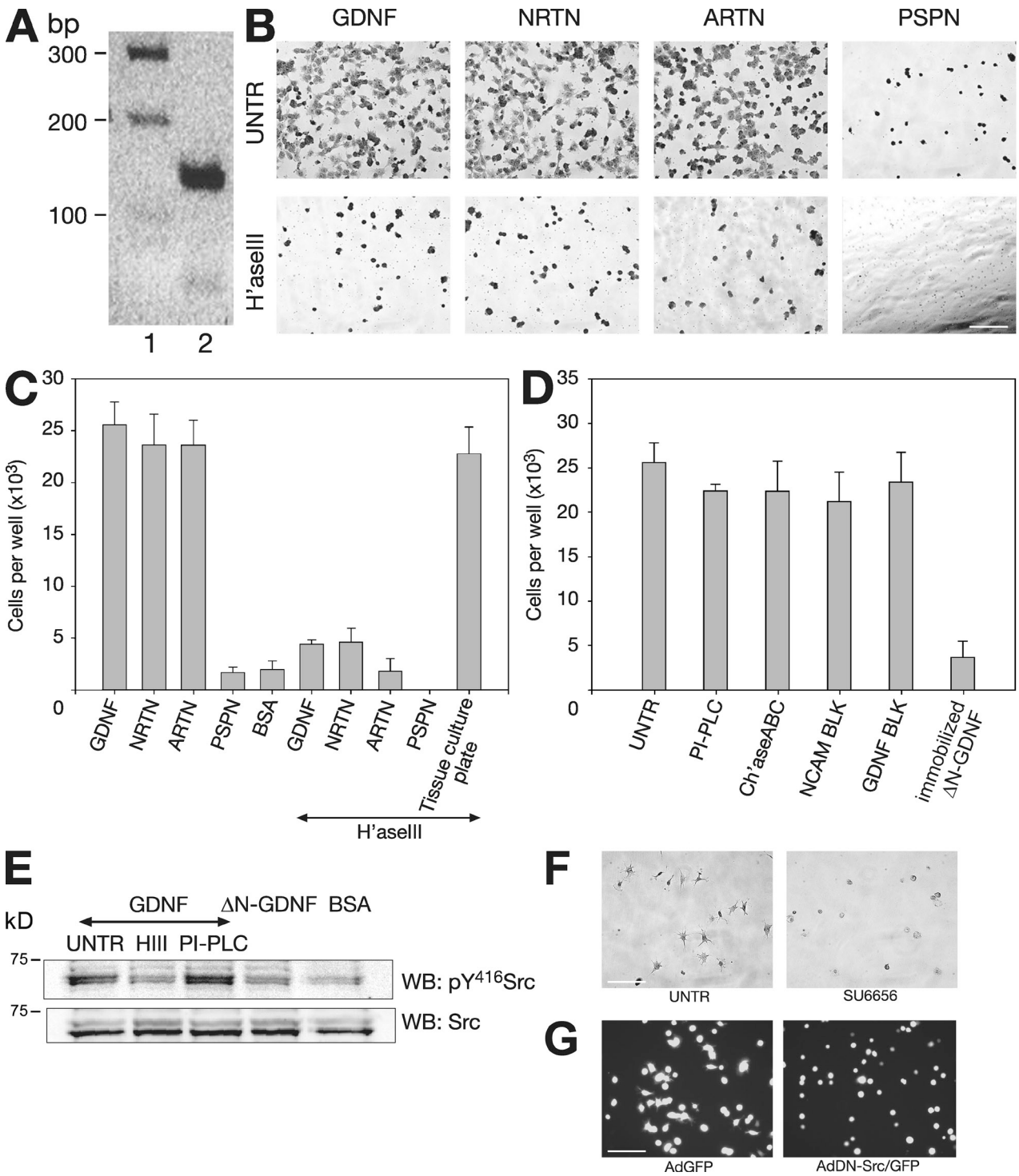

Figure 3. **GDNF, NRTN, and ARTN induce SHEP cell adherence and SFK activation in an HSPG-dependent manner.** (A) RT-PCR of the cDNA from SHEP cells with syndecan-3–specific primers. The resulting 140-bp band represents a syndecan-3 mRNA-derived PCR product (lane 2). (lane 1) Molecular weight markers with sizes in bp. (B) Crystal violet staining of SHEP cells plated on immobilized GDNF, ARTN, NRTN, and PSPN with or without heparinase III (H'aseIII) pretreatment. (C) Quantification of attached SHEP cells on immobilized GFLs. Some cells were treated with heparinase III. Quantification also includes controls with cell attachment on BSA and attachment of cells treated with heparinase III on tissue culture plates. (D) Quantification of SHEP cell adherence to immobilized GDNF and ΔN-GDNF. Cells were plated on GDNF untreated, or they were pretreated with PI-PLC, chondroitinase ABC (Ch'ase ABC), NCAM function-blocking antibodies (NCAM BLK), or GDNF function-blocking antibodies (GDNF BLK). (C and D) Error bars show SEM from three independent assays. (E) Western blot (WB) for activated SFK in lysates from SHEP cells plated on GDNF, ΔN-GDNF, or BSA. In control experiments, cells plated on GDNF were treated with heparinase III (HIII) or PI-PLC. Western blots were probed with anti-pY^{418}Src (top) or anti-Src (bottom) antibodies. (F) SHEP cell adherence and spreading on immobilized GDNF in the absence or presence of 2 μM SFK inhibitor SU6656. Cell spreading on immobilized GDNF was impaired in the presence of the inhibitor, whereas adherence of SHEP cells was not significantly affected by SU6656. (G) Adherence and spreading of SHEP cells infected with adenovirus expressing GFP (AdGFP) or dominant-negative Src (AdDN-Src/GFP) on immobilized GDNF. Transduction of cells with AdDN-Src/GFP resulted in SHEP's failure to spread on immobilized GDNF. GFP-expressing adenovirus did not affect SHEP cell spreading on the GDNF matrix. Untreated, UNTR. Bars, 100 μM.

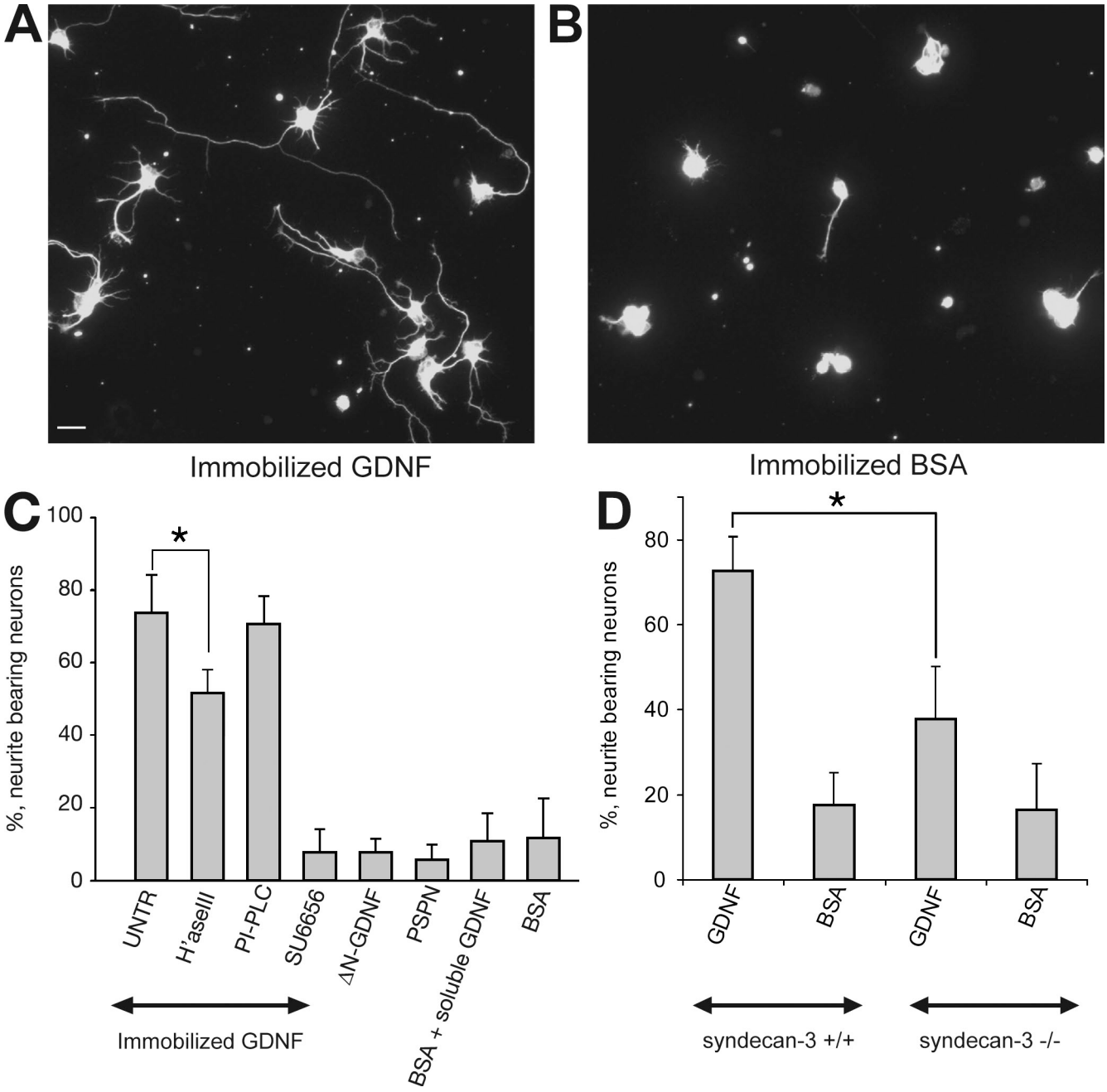

Figure 4. **Immobilized GDNF induces neurite outgrowth in rat embryonic hippocampal neurons.** (A) Neurite outgrowth in E17 rat hippocampal neurons on immobilized GDNF. Neurons are stained with tubulin-βIII antibodies. Bar, 20 μM. (B) Neurite outgrowth in hippocampal neurons plated on BSA. Neurons are stained with tubulin-βIII antibodies. (C) Quantification of neurite outgrowth on immobilized GDNF, ΔN-GDNF, PSPN, and BSA. Neurons plated on GDNF were untreated (UNTR) or preincubated with heparinase III (H'aseIII), PI-PLC, or 2 μM SFK inhibitor SU6656. As a control, soluble GDNF was added to neurons grown on BSA. Error bars show SEM from three to five independent experiments (*, $P < 0.05$). (D) Quantification of neurite outgrowth on immobilized GDNF and BSA from wild-type (syndecan-$3^{+/+}$) and syndecan-3–deficient (syndecan-$3^{-/-}$) neurons. Error bars show SEM from three independent experiments (*, $P < 0.05$ by paired *t* test).

important for these processes, we used rat embryonic (embryonic day 17 [E17]) hippocampal neurons, which express syndecan-3 (Raulo et al., 1994; Lauri et al., 1999), GDNF, and very little RET (Trupp et al., 1997). When grown on HB-GAM substrate, these neurons extend numerous neurites with prominent syndecan-3 localization in varicosities and growth cones (Raulo et al., 1994). Immobilized GDNF also stimulated neurite outgrowth in E17 hippocampal neurons (Fig. 4 A). Neurite outgrowth quantification showed that the process was neither affected by PI-PLC treatment (Fig. 4 C) nor by NCAM function-blocking antibodies (not depicted), excluding the involvement of conventional receptors. The number of neurite-bearing neurons was significantly lower after treatment of cells with heparinase III, and neurons failed to form processes on nonheparin-binding substrates such as ΔN-GDNF, PSPN, and BSA (Fig. 4, B and C), confirming the role of HS chains in the interaction. Likewise,

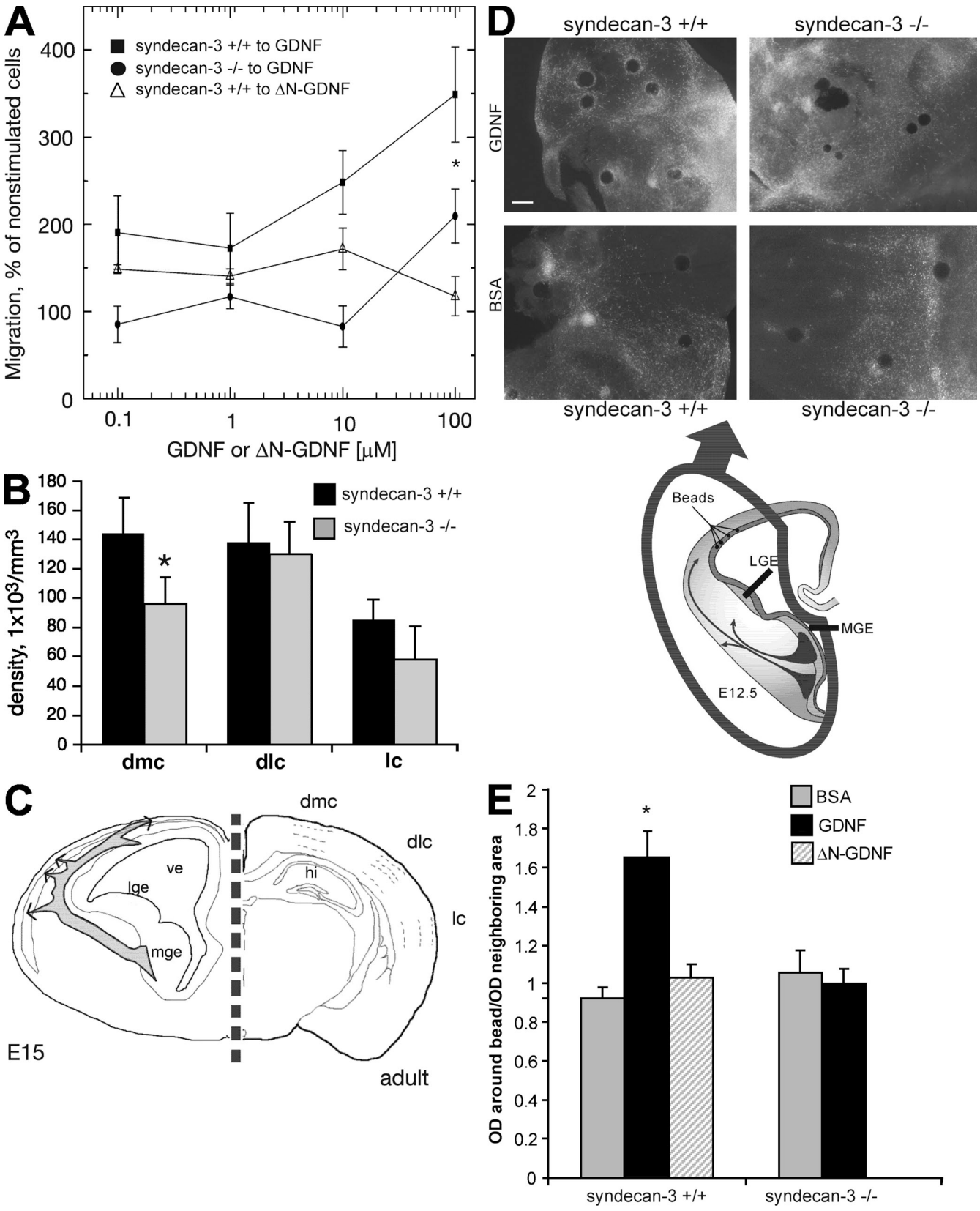

Figure 5. **GDNF stimulates migration of embryonic mouse cortical neurons via syndecan-3.** (A) E15 cortical neurons in a modified Boyden chamber migrate toward wtGDNF (squares) but not toward ΔN-GDNF (triangles). Cortical neurons from syndecan-3–deficient mice (circles) migrate toward GDNF less efficiently than wild-type neurons. Error bars show SEM from three independent experiments. (B) Adult syndecan-3–deficient mice have less GABAergic neurons in the cerebral cortex. GABAergic cell density is significantly smaller in the most dorsal parts of the cortex (dmc) in syndecan-3 knockout brains (gray bar) compared with wild type (black bar). The cell density is almost identical to the wild type in the most lateral parts of the cortex (dlc and lc). dmc, dorsomedial cortex; dlc, dorsolateral cortex; and lc, lateral cortex. Error bars show SEM. (A and B) *, $P < 0.05$. (C) A schematic presentation shows

the SFK inhibitor SU6656 prevented neurite outgrowth (Fig. 4 C). Soluble GDNF added to neurons grown on the BSA matrix failed to induce neurites. Because both ΔN-GDNF and wild-type GDNF (wtGDNF) are basic proteins, we suggest that the observed difference in neurite outgrowth is not attributed to their electrostatic properties and is specific for the heparin-binding tail of GDNF. We conclude that the interaction between HSPGs and immobilized GDNF is involved in the induction of neurite formation by GDNF in rat embryonic hippocampal neurons and that SFK activation is crucial for this process.

Because syndecan-3 is the only HSPG known to transmit extracellular signals via SFKs (Rauvala et al., 2000), we examined the involvement of syndecan-3 in GDNF-induced neurite outgrowth by performing the assay with E16 murine hippocampal neurons from wild-type and syndecan-3 knockout animals (Reizes et al., 2001). At least 70% of neurons from wild-type mice developed long neurites when grown on immobilized GDNF, whereas the number of neurite-bearing cells was significantly reduced in the culture of syndecan-3–deficient neurons (Fig. 4 D).

GDNF interaction with syndecan-3 drives migration of embryonic cortical neurons

Tangential migration and differentiation of cortical GABAergic neurons during embryonic development depends on GDNF, although cortical neurons lack RET and NCAM (Fig. S3; Pozas and Ibáñez, 2005). In the transfilter cell migration assay, GDNF stimulated substantial migration of embryonic cortical cells compared with the tissue culture–treated adhesive surface or the polycationic filter surface (Fig. 5 A). In contrast, ΔN-GDNF did not induce migration in this assay. Likewise, GDNF-stimulated migration of syndecan-3–deficient (Reizes et al., 2001) embryonic cortical neurons was strongly impaired (Fig. 5 A). Interestingly, the highest concentration of GDNF could also stimulate migration of the knockout neurons, indicating the potential involvement of other GDNF receptors, e.g., GFR-α1, as was previously suggested (Pozas and Ibáñez, 2005).

To establish in vivo relevance of GDNF interaction with syndecan-3, we performed a redirected GABAergic neuron migration assay in live brain explants. Agarose beads were soaked in various proteins and placed on top of E12.5 brain explants containing part of the medial ganglionic eminence (GE [MGE]) and developing cortex (Fig. 5 D, drawing; and Fig. S4). After 56 h of incubation, the explants were fixed, and GABAergic neurons were identified by anticalbindin staining. We found that GABAergic neurons were attracted by GDNF beads but not by beads containing BSA, ΔN-GDNF, or laminin (Fig. 5, D and E; and Fig. S4). Neurons from syndecan-3 knockout animals failed to migrate toward GDNF but efficiently migrated toward brain-derived neurotrophic factor (BDNF) beads (Fig. 5, D and E; and Fig. S4). These facts suggest that the promotion of GABAergic cell migration is mediated by GDNF–syndecan-3 interaction and that this effect is specific.

Furthermore, we found that at E15, the number of calbindin-positive cells was significantly increased in the intermediate zone (IZ) of the GEs of syndecan-3–deficient embryos compared with the wild types (Fig. 6, A, D, and G). The intensity of the general neuronal marker Tuj1 was not altered in syndecan-$3^{-/-}$ sections (Fig. 6, B, E, and H). We therefore reasoned that the accumulation of GABAergic precursors in GEs may be caused by migration defects in mutant embryos. Because, after proliferation, the immature interneurons migrate tangentially from the GE to colonize the cortical plate, we assumed that the accumulation of GABAergic cells in the IZ during embryogenesis would result in interneuron deficiency in the adult cortex.

Consistently, the density of GABA-immunopositive cells was significantly lower in layers II–IV of the dorsomedial cortex of adult syndecan-3–deficient mice (Fig. 5, B and C). The dorsomedial cortex is the most distant area along the tangential migration route from the place of interneuron origin. We found no difference in the width of the cortical layers (not depicted), and cortical areas proximal to the source of interneurons did not show any clear difference in the density of GABAergic neurons (Fig. 5, B and C).

Importantly, no signs of increased apoptosis were found in the syndecan-3–deficient brains (Hienola et al., 2006). Thus, the data indicate that the GDNF–syndecan-3 interaction plays a distinctive role in cerebral cortex development by promoting migration of GABAergic neurons.

Discussion

Brain development is remarkably dependent on HSPGs. Neural-specific conditional knockout of EXT1, the enzyme that catalyzes HS polymerization, showed that this protein is vital for brain patterning and axon scaffold formation in the forebrain (Inatani et al., 2003). HSPGs support activity of various growth factors, receptors, and guidance molecules during development, including FGFs or Robo-Slit signaling (Van Vactor et al., 2006). Here, we present evidence that also some GFLs could use HSPGs as their signaling partners. In particular, GDNF, which has been recently implicated in embryonic cortical development (Pozas and Ibáñez, 2005), could signal via brain HSPG

the cortical areas where the density measurements were made. Arrows show the tangential migration route in E15 mice. The dotted line separates the schemes of an adult and E15 brain. lge, lateral ganglionic eminence; mge, medial ganglionic eminence; ve, ventricle; and hi, hippocampus. (D) Assay for redirected migration assay of GABAergic neurons. (top) GDNF attracts embryonic (E12.5) calbindin-positive neurons in living brain explants from wild-type (syndecan-$3^{+/+}$) mice but not from syndecan-3 knockout explants (syndecan-$3^{-/-}$). BSA fails to attract neurons. Bar, 200 µM. (bottom) The scheme of neuronal migration in the mouse brain of E12.5 (modified from Marín and Rubenstein, 2003). The explants were prepared from the area marked by the gray oval. Agarose beads soaked in various proteins were placed on top of the ventricular zone to stimulate neuronal migration. (E) Quantification of the migration assay. GDNF attracts GABAergic neurons from wild-type living explants (syndecan-$3^{+/+}$) but fails to do so in syndecan-3–deficient explants (syndecan-$3^{-/-}$). Neither ΔN-GDNF nor BSA attracted neurons. For the evaluation of GABAergic neurons in syndecan-$3^{-/-}$ animals, six mice (12 brain slices) were processed. For the measurements in syndecan-$3^{+/+}$ animals, the brains from six mice (18 brain slices) were processed. Error bars show SEM (*, $P < 0.01$).

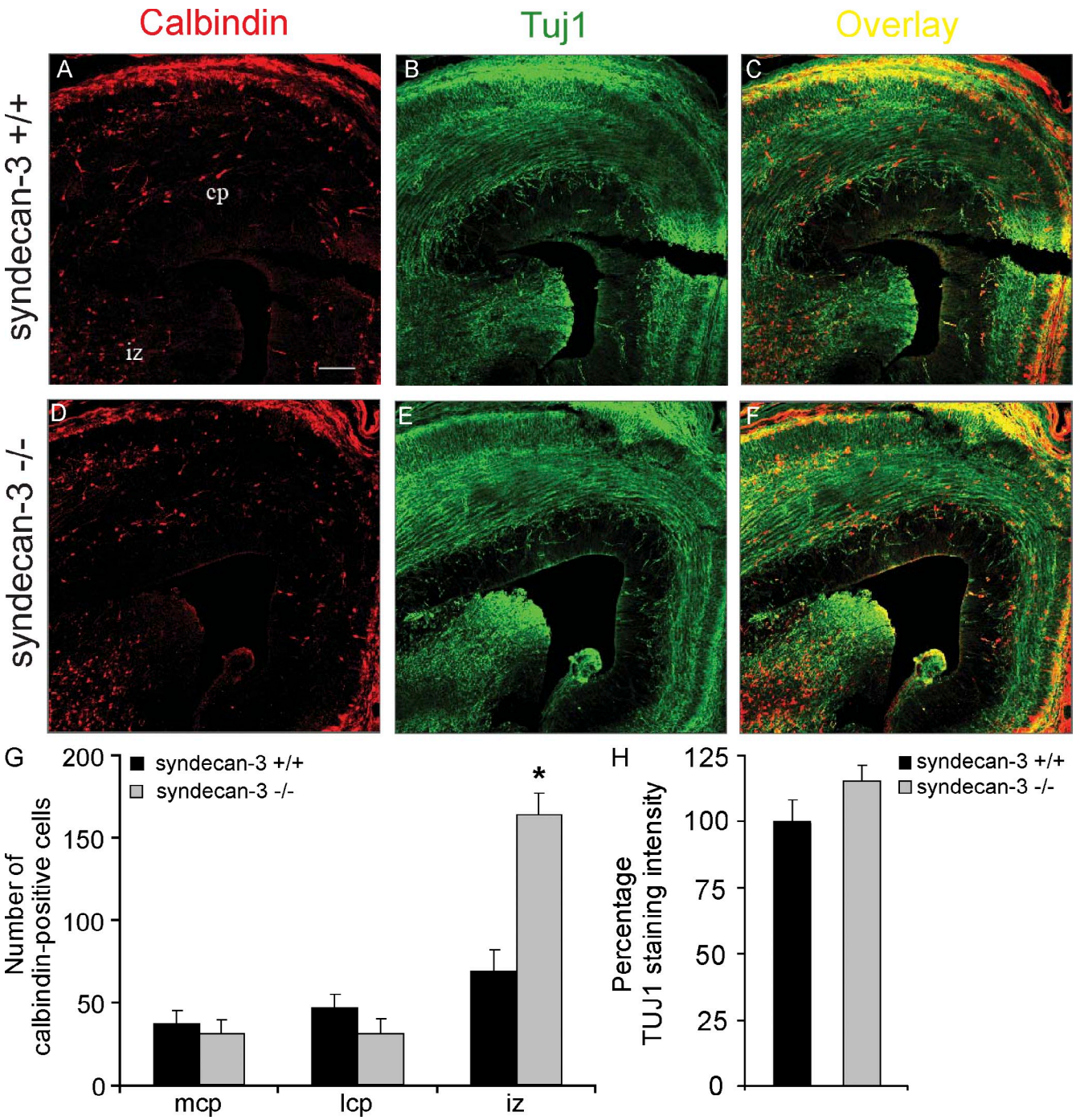

Figure 6. **Syndecan-3 is required for the migration of immature interneurons in the developing telencephalon.** (A–F) Coronal sections through the developing telencephalon of wild-type (syndecan-3$^{+/+}$, A–C) and syndecan-3$^{-/-}$ embryos (D–F) showing calbindin and Tuj1 immunostaining. (C and F) Merged images of calbindin and Tuj1 stainings. (G) The graph depicts the mean number of calbindin-positive cells in the medial (mcp) and lateral (lcp) cortical plate (cp) and in the intermediate zone (iz) of the GE. (H) The intensity of Tuj1 staining is not altered in syndecan-3–deficient brains. (G and H) Error bars show SEM of three embryos (syndecan-3$^{+/+}$, $n = 3$; and syndecan-3$^{-/-}$, $n = 3$). *, $P < 0.01$. Bar, 80 µm.

syndecan-3 in cortical neurons, which lack the canonical GFL receptors RET and NCAM (Pozas and Ibáñez, 2005).

We find that GDNF, ARTN, and NRTN bind heparin with K_ds in the range of 10–50 nM, which is comparable with other high affinity heparin-binding molecules, such as FGFs or HB-GAM. More significantly, heparin-binding GFLs also bind the HSPG syndecan-3 isolated from the brain with similar affinity, suggesting that syndecan-3 could be their natural binding partner in the developing brain. This is supported by the known expression patterns of syndecan-3, GDNF, and NRTN during brain development. Syndecan-3 associates with growing axons and neural processes and is found in most of the major neuronal migration routes (Nolo et al., 1995; Kinnunen et al., 1999). GDNF and NRTN are found in the cortex, striatum, and olfactory bulb. In these areas, they are expressed by the glial guidance structures, such as radial glia, and, thus, may provide cues

for migrating cells and growing axons (Golden et al., 1999; Ikeda et al., 1999; Koo and Choi, 2001). Our present findings indicate that the GDNF–HSPG interaction can stimulate neurite outgrowth and migration of primary neurons in vitro and implicate syndecan-3 as the GDNF signaling partner in the brain.

Our results also show that PSPN may lack the ability to bind HSPGs in the ECM, raising an intriguing possibility that, unlike other GFLs, PSPN could diffuse longer distances in tissues reaching body fluids. Therefore, PSPN may act as a circulating hormone-type growth factor, offering an explanation for why PSPN and its specific coreceptor GFR-α4 are expressed in different tissues (Lindahl et al., 2000).

Although syndecan-3 is the likely binding partner for immobilized GFLs in the nervous system, different members of the syndecan family could be signaling receptors and/or coreceptors for GFLs in other tissues. For example, syndecan-1 could be the GDNF coreceptor in the developing kidney. Notably, targeted disruption of *2-O-sulfotransferase* or *glucuronyl C5-epimerase* genes, which encode enzymes important for HS chain maturation, lead to renal agenesis in mice (Bullock et al., 1998; Li et al., 2003). This phenotype is markedly similar to GDNF-deficient mice that also lack kidneys (Moore et al., 1996; Pichel et al., 1996).

Syndecans, in general, can act as coreceptors for various growth factors or ECM molecules. Although they lack intrinsic kinase or phosphatase activity, their cytoplasmic domains can associate with cytoskeletal proteins or protein kinases, making it possible to transmit extracellular signals to the cytoskeleton via SFK–cortactin, ezrin–cdc42, and calcium/calmodulin-dependent serine protein kinase–protein 4.1 pathways (Rauvala et al., 2000; Yoneda and Couchman, 2003). Syndecan-3 is unique, as it is the only syndecan shown to signal independently of other receptors by activating SFKs (Raulo et al., 1994; Kinnunen et al., 1998). Our data indicate that immobilized GDNF, NRTN, and ARTN can also stimulate cell adhesion and spreading via syndecan-3 without involvement of their conventional receptors. We show that GDNF triggers SFK signaling in an HSPG-dependent manner and that the SFK activity is required for cell spreading but not for initial attachment. Based on these findings, we speculate that the interaction between immobilized GFLs and syndecans first leads to the receptor anchoring to the GFL matrix and then subsequent signaling activates SFKs, leading to full spreading. The intermediate step could involve syndecan oligomerization triggered by GFL binding. GDNF, NRTN, and ARTN all have at least one putative heparin binding site. In particular, the primary HS/heparin binding site is at the N terminus of GDNF (Fig. S2), which is highly flexible and unique to GDNF and is absent in other GFLs. The N terminus of GDNF is available for interaction with HSs both as a free and immobilized protein (Table S1). In NRTN and ARTN, the HS binding sites are likely to be located in the central region. Because all GFLs are produced as covalently linked homodimers, they contain two heparin binding sites capable of linking neighboring syndecan molecules. Indeed, the high molecular weight band detected after chemical cross-linking in C6 glioma cells could correspond to syndecan-3 oligomers in complex with GDNF (Fig. 2 B). Syndecan-3 oligomerization was also detected in our FRET experiments (Fig. 2 D).

Interestingly, because syndecan-3 has several HS chains, one molecule of syndecan-3 can simultaneously bind multiple GFL homodimers. Thus, compared with the GFR-α–RET receptor complex, which binds one GFL dimer with very high affinity (0.01–0.5 nM; Cik et al., 2000; Leppänen et al., 2004), syndecan-3 is a high affinity/high capacity receptor for GFLs.

For secreted molecules, their ability to bind heparin is often associated with localization in the ECM. Our current work also supports the notion that GDNF is localized predominantly in the ECM and on the cell membrane (Fig. 2 C). Interaction with matrix HSPGs could dramatically change the properties and distribution of the heparin-binding GFLs. By analogy with other heparin-binding proteins, ECM could be the local high capacity store for GFL, participate in generation of GFL gradients, thus determining their precise spatiotemporal positioning, protect GFLs from proteolysis (Hynes, 1999; Geiger et al., 2001), or concentrate and present GFLs to their conventional GFR-α–RET receptors (Sariola and Saarma, 2003).

It has been shown previously that coinfusion of heparin with GDNF, NRTN, or ARTN into rat striatum markedly increased their biodistribution (Hamilton et al., 2001), potentially leading to greater therapeutic effects of GFLs. Our findings indicate that this was because heparin prevented GFL binding locally to syndecan-3 or other HSPGs in the brain ECM. This knowledge may allow a breakthrough in the successful therapeutic use of GFLs by promoting the generation of variants lacking affinity to HSPGs and, thus, with increased biodistribution and bioavailability.

In our assays, immobilized, but not soluble, GDNF induced spreading and robust (within the first hours of experimentation) neurite outgrowth in embryonic hippocampal neurons (Fig. 4). Syndecan-3 was required for efficient neurite outgrowth (Fig. 4 D), and because SU6656 caused a drastic reduction in the number of neurites (Fig. 4 C), we assumed that SFK signaling was also involved in GDNF-induced neuritogenesis. We were unable to observe Src kinase activation in hippocampal neurons by Western blotting as we did in the SHEP cells (Fig. 3 E). However, we found that, in PC6-3 pheochromocytoma cells, 30-min pretreatment with 2 μM SU6656 efficiently blocked both neurite outgrowth and Src activation (unpublished data). Embryonic hippocampal neurons express negligible levels of RET, and neither release of GPI-anchored GFR-α1 by PI-PLC nor NCAM-blocking antibodies had any effect on the GDNF-induced neurite outgrowth. In contrast to our data, Paratcha et al. (2003) found that NCAM-blocking antibodies reduced GDNF-induced neurite outgrowth in hippocampal neurons. This discrepancy could be a result of Paratcha and co-authors measuring the length of neurites initiated by GDNF, whereas we analyzed the number of neurons bearing neurites. Therefore, we studied the initiation of neurite outgrowth rather than the progression of already formed neurites. We have also observed that, in syndecan-3$^{-/-}$ neurons, immobilized GDNF had residual activity in promoting the neurite outgrowth (Fig. 4 D). We have speculated that this effect may be caused by GFR-α1, which was shown to be a ligand-induced cell adhesion molecule (Ledda et al., 2007)

The possible involvement of syndecan-3 in GDNF signaling, supported by our in vitro data, could be highly relevant

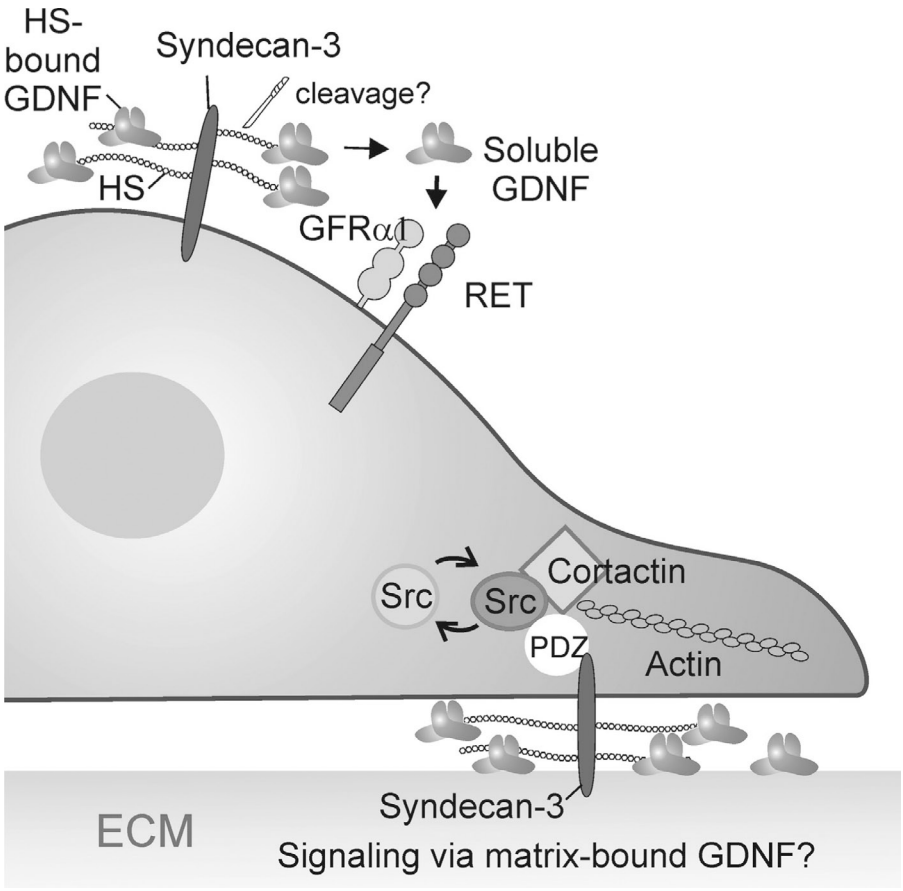

Figure 7. **Hypothetical model of GDNF signaling mediated by syndecan-3.** Matrix-bound GDNF may directly induce syndecan-3 signaling via interaction with heparan sulfate (HS) chains of the receptor. Alternatively, syndecan-3 can modulate RET (or NCAM) signaling induced by soluble GDNF.

during cortical development. During cerebral cortex formation, inhibitory GABAergic interneurons originate mainly from the MGE and then migrate tangentially into the developing cortical layers (Fig. 5 C; Marín and Rubenstein, 2003). Recently, mouse cortical GABAergic neurons were shown to migrate along the GDNF gradient from the MGE toward the cortex. These neurons lack RET and NCAM, and so it has been suggested that an alternative GDNF receptor system drives their migration (Pozas and Ibáñez, 2005). Detailed analysis by Pozas and Ibáñez (2005) demonstrated that GDNF and GFR-α1 knockout animals have significantly fewer GABAergic neurons in their cortex, whereas mice lacking RET and NCAM have the normal number of GABAergic cortical neurons, indicating that GDNF acts as a chemoattractant for GABAergic cortical neurons via a novel RET- and NCAM-independent pathway.

Here, we demonstrate that syndecan-3 mediates GDNF-induced migration and differentiation (Fig. S3) of cortical neurons and, specifically, of the GABAergic population. We used a transfilter migration assay for embryonic cortical neurons, whereas a specific GABAergic neuronal population was studied by quantifying their redirected migration in living explants. In both assays, migration was specifically stimulated by GDNF but not by ΔN-GDNF, which cannot bind syndecan-3 (Fig. 5, A, D, and E). Syndecan-3–deficient neurons failed to migrate toward GDNF in both assays, but they were still capable of migration toward laminin in the transfilter assay (unpublished data). Knockout neurons also migrated toward neurotrophin BDNF, which signals via TrkB and p75 receptors, in the migration assay (Fig. S4). These facts further support the specific role of syndecan-3 in the GDNF signaling pathway.

After leaving GE, the immature interneurons migrate tangentially to colonize the cortical plate. We detected the accumulation of the GABAergic cells in the IZ of the GE of syndecan-3 knockout mice, suggesting the migratory defect in these cells (Fig. 6). Other cells (Tuj1 stained) did not accumulate in the IZ, suggesting that, in the tangential migratory stream, the effect is confined to the interneurons. It is unclear what restricts the effects of GDNF to the population of GABAergic cells. We suggest that GFR-α1 expression is important for GDNF to exert its effects in vivo (Pozas and Ibáñez, 2005).

Consistently, we can detect a clear drop in the density of GABAergic cells in the dorsal cerebral cortex of the adult syndecan-3–deficient mice (Fig. 5 B), and as neural proliferation and differentiation are normal in syndecan-3 knockout mice (Hienola et al., 2006), we conclude that, in the absence of syndecan-3, migration of GABAergic neurons is defective. The brain phenotype of syndecan-3–deficient mice is markedly similar to the GDNF knockout phenotype found by Pozas and Ibáñez (2005), suggesting a likely physiological interaction between these molecules.

In summary, this work identifies syndecan-3 as a novel receptor for immobilized GDNF, NRTN, and ARTN, which is fundamentally different from that for diffusible GFLs. GFL interaction with syndecan-3 (or a receptor complex consisting of syndecan-3 and an unknown signal-transducing molecule) and with GFR-α–RET or GFR-α–NCAM induces distinct biological

effects (Fig. 7). Our results clearly show that, in the absence of conventional receptors, HSPG syndecan-3 is required for immobilized GDNF-induced intracellular signaling leading to the activation of SFKs, triggering cell spreading, neurite outgrowth, and neuronal migration. Moreover, GDNF interaction with syndecan-3 is likely to be important for brain cortex development.

Our simplified model (Fig. 7) illustrates the idea that the interaction of GDNF, NRTN, and ARTN with the HS of syndecan-3 can concentrate and present GFLs to their conventional receptors GFR-α–RET or GFR-α1–NCAM. The model predicts a new regulatory step in GFL signaling: cleavage of HS or the syndecan-3 ectodomain to regulate the release of diffusible GFLs required for GFR-α–RET receptor activation. We propose that the long-range (chemotactic) signals exerted by diffusible GFLs are mediated by GFR-α–RET, whereas the short-range effects are transduced via syndecan-3. Our study indicates, for the first time, that a growth factor may activate signal transduction through HSPG and that the same signaling molecule, GDNF, elicits different biological effects via different receptors when immobilized or as a free diffusible protein (Fig. 7).

Materials and methods

Cell cultures and reagents

The rat glioma C6 cell line and the mouse neuroblastoma cell line Neuro2a were obtained from American Type Culture Collection. Early passage RET-deficient human SHEP cells were provided by M. Billaud (Centre National de la Recherche Scientifique, Lyon, France). MG87-RET cells were obtained from C.F. Ibáñez (Karolinska Institute, Stockholm, Sweden). Rat hippocampal neurons were isolated from E17 embryos. Mouse cortical neurons were isolated from E15 embryos. The use of experimental animals was approved by the Committee for Animal Experiments of the University of Helsinki and the chief veterinarian of the County Administrative Board (permissions HY 173–04 and 55–06 and ESLH-2006-04080/Ym-23). Low molecular weight heparin, heparin-BSA, ethyl-dimethyl-aminopropyl-carbodimide/*N*-hydroxysuccinimide cross-linker, lactoperoxidase, PI-PLC, chondroitinase ABC, globulin-free BSA, and cell culture–tested BSA were purchased from Sigma-Aldrich. SU6656 was bought from EMD. Heparinase III was obtained from Seikagaku Corp. (Seikagaku's trademark for this product is Heparitinase I). The dominant-negative Src adenoviral construct was a gift from D. Kaplan (Hospital for Sick Children, Toronto, Canada). Desulfated heparins were provided by R. Takano (Okinawa National College of Technology, Okinawa, Japan). G90 antibodies were provided by R. Marino (Amgen, Inc., Thousand Oaks, CA). Tritium-labled heparin was a gift from U. Lindahl (University of Uppsala, Uppsala, Sweden).

GFL iodination and binding to heparin-Sepharose

GDNF, ARTN, NRTN, and PSPN were purchased from PeproTech or R&D Systems. GFLs were enzymatically labeled with carrier-free [^{125}I]NaI (GE Healthcare) by the lactoperoxidase method to a specific activity of 100,000–200,000 cpm/ng as described previously (Lindahl et al., 2001). 15,000–20,000 cpm of iodinated GFLs together with 10 µg of the same unlabeled protein as a carrier were injected into a 1-ml heparin–Sepharose column (GE Healthcare) in phosphate buffer, pH 7.2, containing 100 mM NaCl and 10 mg/ml BSA. After washing with five volumes of the same buffer, 2 ml of step-wise elution was performed with increasing NaCl concentration. The resulting fractions were counted on a scintillation counter (Rackbeta 1214; LKB/Wallac).

SPR studies

The affinities of GFLs for heparin and heparin-like molecules were determined by SPR using the IAsys system (Thermo Fisher Scientific). Planar aminosilane cuvettes (Thermo Fisher Scientific) were used to avoid problems with mass transport, which occur frequently with matrix surfaces. In the initial approach, heparin-BSA was immobilized to the cuvette surface according to the manufacturer's instructions, and different ligand concentrations were used to determine association (k_a) and dissociation (k_{dis}) rates using the IAsys Fastfit software. The K_d was determined from the binding dynamics as $K_d = k_a/k_{dis}$ or from equilibrium response (R) using a simple Langmuir fit, $R = (R_{max} \times C)/(K_d + C)$, in which C is the ligand concentration. Because all ligands except PSPN displayed background binding to a control BSA cuvette, K_ds were also determined in a system in which GDNF, ARTN, NRTN, and PSPN were immobilized to the aminosilane surface and different concentrations of heparin were presented in a solution. The K_ds were determined from binding dynamics and equilibrium response. The same cuvettes were used to test binding of HSPG syndecan-3, which was purified as an ectodomain from early postnatal rat brains by HB-GAM affinity chromatography (Raulo et al., 1994).

Specifically desulfated heparins (Takano et al., 1998) were used to assess the involvement of different sulfate groups in the GDNF–heparin interaction by following direct binding to the GDNF cuvette or by competing out GDNF binding to the heparin-BSA cuvette. K_ds were determined from direct binding using increasing GDNF concentrations and by fitting the data to $R = (R_{max} \times C)/(K_d + C)$ for heparin. For desulfated heparins, the best fit was achieved using the equation $R = (R_{max1} \times C)/(K_{d1} + C) + (R_{max2} \times C)/(K_{d2} + C)$, in which K_{d1} and K_{d2} are apparent K_ds derived for two heparin sites of different affinities with maximum equilibrium response R_{max1} and R_{max2}, respectively. The presence of a higher affinity component (K_{d1} of 30–40 nM) for all desulfated heparins could be a result of incomplete desulfation and/or the presence of residual sites with high affinity for GDNF.

Chemical cross-linking and immunoprecipitation

Glioma C6 cells were plated on 6-well plates and grown to 70% confluence. Cells were incubated with 1 nM ^{125}I-GDNF for 2 h in binding buffer (DME, 0.2% BSA, and 15 mM Hepes, pH 7.2) on ice. The unbound ligand was removed by washing three times with ice-cold PBS. The chemical cross-linker ethyl-dimethyl-aminopropyl-carbodimide supplemented with *N*-hydroxysuccinimide was incubated with cells for 20 min at room temperature in PBS. The reaction was quenched with TBS for 15 min, and cells were lysed in the lysis buffer (TBS, 1% Triton X-100, 1% NP-40, 2 mM EDTA, 1 mM PMSF, and protease inhibitor mixture [Complete; Roche]). Cell lysates were immunoprecipitated with antisyndecan-3 antibodies (Nolo et al., 1995) and resolved on 7.5% SDS-PAGE. Autoradiography was performed with an image analyzer (BAS1500; Fujifilm). For heparinase III or PI-PLC treatment, cells were incubated with 10 mU/ml heparinase III or with 1 U/ml PI-PLC, respectively, for 1 h at 37°C and 5% CO_2 before ^{125}I-GDNF addition.

RT-PCR

RNA from SHEP cells was isolated using RNAwiz (Applied Biosystems). First strands were built with random primers using Superscript II (Invitrogen). 35 cycles of PCR were performed with 5′-ATGGCCATTGCTTACCTGG-3′ as a forward primer for syndecan-3 and 5′-AAGCGCATGGCTGTCTCAA-3′ as a reverse primer. DyNAzyme II (Finnzymes) polymerase was used, and the annealing temperature was 58°C.

Separation of membrane-bound and ECM-bound protein fractions of mouse organs

Postnatal day (P) 9 mouse brains and kidneys were dissociated in 1.5 ml of 10-mM Tris-HCl, pH 7.5 (containing protease inhibitor mix, 1 mM EDTA, and 1 mM PMSF), by passing them through a 20-gauge needle on ice. After 10-min incubation on ice, insoluble material was spun down at 13,000 rpm in a tabletop centrifuge for 60 min at 4°C. The supernatant was collected and labeled as the ECM fraction. The pellet was dissolved in PBS with 1% NP-40 for 30–60 min on ice and centrifuged at 13,000 rpm for 90 min at 4°C. The supernatant was collected and labeled as the membrane fraction. Volumes in both the ECM and membrane fractions were equalized. Fractions were separated on 15% SDS-PAGE, and Western blots were stained either with GDNF antibodies (Santa Cruz Biotechnology, Inc.) or with HB-GAM antibodies (Rauvala, 1989). Anti–rabbit horseradish peroxidase–conjugated secondary antibodies (GE Healthcare) were used for the primary antibody detection. For imaging chemiluminescence, the LAS-3000 imaging system (Fujifilm) was used.

FRET experiments

To study GDNF-induced syndecan oligomerization, we tagged rat syndecan-3 with YFP and CFP. The sequences were placed immediately after the transmembrane domain of the receptor in the cytosolic part after Tyr409 residue.

The constructs were transfected into HEK293T cells seeded on 20 µg/ml poly-L-lysine–coated 35-mm glass-bottom culture dishes (MatTek) with FuGene 6 (Roche). Cells were incubated for a few hours in serum-free medium before FRET measurements at 37°C and 5% CO_2. During the stimulation with 100 ng/ml GDNF for up to 40 min and during image acquisition, the temperature was decreased to 22–24°C.

FRET measurements were performed as described previously (Hienola et al., 2006). In brief, FRET was quantified with three filter sets: CFP channel, excitation (EX) D436/20×, emission (EM) D480/40m, and dichroic longpass 455 (DCLP); FRET channel, EX D436/20×, EM D535/30m, and DCLP 455; and YFP channel, EX HQ500/20×, EM HQ535/30m, and DCLP 515 (Chroma Technology Corp.).

Images were recorded in live transfected cells using Cell^R Imaging Systems (Olympus) with a 60× objective. The background subtraction was made before FRET calculations.

All images were corrected for cross talk from CFP and YFP channels using the linear spectral unmixing formula Fc = FRET channel − a × CFP channel − b × YFP channel, in which a and b are correction factor values for CFP and YFP, which were found to be 0.4235 ± 0.018 (n = 25) and 0.0238 ± 0.0007 (n = 21), respectively (described in the following paragraph).

CFP and YFP were expressed separately and for each fluorophore. The emission from the FRET channel was divided by the emission measured with either the CFP or YFP channels: a = FRET/CFP (0.4235 ± 0.018) and b = FRET/YFP (0.0238 ± 0.0007). In Fig. 2 D, FRET-corrected images were displayed in pseudocolors (red areas designate high values of FRET, and blue areas designate low values of FRET).

Cell adhesion assay

Cell adhesion assays were essentially performed as described previously (Weinacker et al., 1994). To prepare protein-coated surfaces, the protein of interest (10 µg/ml in PBS) was applied to 96-well ELISA plates (Greiner) or to glass coverslips for 12–18 h at 4°C. After incubation, the surfaces were washed with PBS and blocked with 1% globulin-free BSA for 2 h. Some GDNF-coated surfaces were incubated with 20 µg/ml G-90 GDNF function-blocking antibodies (Xu et al., 1998) for 2 h at room temperature.

Subconfluent SHEP cells were harvested in PBS supplemented with 10 mM EDTA for 5 min at 37°C. Cells were washed with incubation buffer (RPMI 1640, 0.2% BSA, and 15 mM Hepes, pH 7.2), and 10,000–40,000 cells per well were plated on the protein-coated surface. Plates were centrifuged for 5 min at 10 g and incubated for 1 h at 37°C in 5% CO_2. After incubation, cells were washed with PBS, fixed with methanol supplemented with crystal violet for 15 min at room temperature, and washed again with PBS. The remaining cells were stained and counted on an inverted microscope (DMIRB; Leica) with a 10× objective in five fields per well, and the resulting cell number was calculated for the whole well. Some cells were pretreated with heparinase III, 1 U/ml PI-PLC, and 0.3 U/ml chondroitinase ABC for 1 h at 37°C in 5% CO_2 or with 20 µg/ml NCAM-blocking antibodies (AB5032; Millipore) for 15–30 min on ice. Live SHEP cells spreading on immobilized GDNF were imaged for 20 min using an imaging system with a digital camera (Imago QE; TILL Photonics) equipped with heating (37°C) and CO_2 supply (5%) chambers.

Src kinase phosphorylation assay

SHEP cells from 10-cm plates were harvested (see the previous paragraph) and plated on GDNF-coated 35-mm petri dishes. Some cells were pretreated with heparinase III and PI-PLC (see the previous paragraph). Cells were allowed to sediment for 10 min at room temperature and then were transferred to 37°C for an additional 15 min. Cells were lysed in the lysis buffer (TBS, 1% Triton X-100, 0.5% deoxycholic acid, 0.1% SDS, 10% glycerol, 1 mM Na_3VO_4, 1 mM PMSF, and protease inhibitor mixture). Lysates were analyzed on 10% SDS-PAGE, and Western blots were stained with anti-pY^{418}Src or anti-pp60Src antibodies (Invitrogen). Some cells were pretreated with heparinase III or PI-PLC.

Isolation and characterization of heparin binding–deficient GDNF mutant

The sequence encoding residues 39–134 of mature human GDNF and an N-terminal FLAG tag was subcloned into the pFASTBAC1 (Invitrogen)-based baculovirus transfer vector pK503.9 (Keinänen et al., 1998; Leppänen et al., 2004). For the baculoviral infection, we used Sf9 insect cells grown in serum-free medium (SF900II; Invitrogen) supplemented with 50 µg/ml gentamicin (Sigma-Aldrich) at 28°C. At 3 d after infection, the soluble secreted ΔN-GDNF was produced at 0.5–1 mg/liter concentration. ΔN-GDNF was purified from culture supernatants by anti-FLAG M1 affinity chromatography (Sigma-Aldrich) followed by cation exchange chromatography on an S column (UNO; Bio-Rad Laboratories). The purity of the GDNF proteins was tested on 15% SDS-PAGE.

RET phosphorylation assay was performed as described previously (Leppänen et al., 2004). In brief, MG87-RET cells (Eketjäll et al., 1999) were transiently transfected with GFR-α1. At 20 h after transfection, media were exchanged for a serum-free DME (Sigma-Aldrich), and cells were starved for 4 h. Then cells were stimulated with 100 ng/ml (3.3 nM) GDNF (PeproTech) or ΔN-GDNF for 10 min at 37°C. Next, cells were lysed on ice, and the lysates were immunoprecipitated with anti-RET antibodies (C-20; Santa Cruz Biotechnology, Inc.). The precipitates were SDS-PAGE resolved, transferred to nitrocellulose membranes, and probed with phosphotyrosine antibodies (4G10; Millipore). To ensure that equal amounts of RET were precipitated in each sample, the filters were stripped and reprobed with antibodies to RET.

Neurite formation in cultured dorsal root ganglion neurons was tested in the presence of ΔN-GDNF or wtGDNF as described previously (Paveliev et al., 2004). In brief, dorsal root ganglia were dissected from thoracic and lumbar spinal segments of 1-mo-old mice (Naval Medical Research Institute). Ganglia were cleaned from nerves and incubated for 20 min in PBS containing 0.15% collagenase I, 0.025% trypsin, and 0.4% BSA at 37°C followed by trituration in HBSS. Cells were plated (culture density of 500–1,000 neurons/cm^2) on glass coverslips. Coverslips were precoated with 1 mg/ml polyornithine overnight at 4°C and then with 100 ng/cm^2 laminin for 4 h at 37°C. Culture medium included 50% F12 and 50% DME supplemented with glutamine, penicillin, streptomycin, and serum substitute containing 0.35% BSA, 60 ng/ml progesterone, 16 µg/ml putrescine, 400 ng/ml L-thyroxine, 38 ng/ml sodium selenite, and 340 ng/ml triiodothyronine. ΔN-GDNF was applied at the time of plating neurons, and cultures were maintained for 12 h after plating. After that, neurons were fixed with 4% PFA in PBS and stained for PGP9.5. The immunostained cultures were viewed using the 20× objective of a fluorescent microscope (Axioplan 2; Carl Zeiss, Inc.).

Neurite outgrowth assay in hippocampal neurons

Hippocampi were dissected from E17 embryonic rat brains under the microscope, transferred to the preparation media (HBSS without Ca^{2+} and Mg^{2+} supplemented with 1 mM sodium pyruvate [Invitrogen] and buffered by 10 mM Hepes, pH 7.2), and then partially digested by papain and triturated in the preparation media supplemented with DNase I. Cells were washed with HBSS containing Ca^{2+} and Mg^{2+} and transferred to the growth media (neurobasal media with B27 supplement, 2 mM L-glutamine, 25 µM glutamic acid, penicillin, and streptomycin [Invitrogen]). For enzymatic treatments, neurons were kept in the growth media supplemented with 0.2% BSA at 37°C for 1 h. SU6656 (Millipore) was used at a 2-µM concentration. After the treatment, cells in the same media were seeded on the protein-coated coverslips (see Cell adhesion assay), and after 10 min, the media were changed for B27-free media. Neurons were incubated at 37°C in 5% CO_2 for 18 h.

For immunocytochemistry, neurons were washed with PBS and fixed with 4% PFA, permeabilized with 0.1% Triton X-100, and stained with rabbit polyclonal antiserum to protein gene product 9.5 (Affiniti), neuron-specific class III tubulin-βIII clone Tuj1 antibodies (BABCO), or with antibodies against the neurofilament triplet 13AA8 (Ylikoski et al., 1993). The secondary antibodies used were Alexa Fluor 488–conjugated goat anti–rabbit or anti–mouse (Invitrogen).

The immunostained cultures were viewed using the 20× objective of a fluorescent microscope (Axioplan 2). Neurons with the processes at least two times longer than cell body diameter were considered process bearing. Three coverslips were used in parallel, and 100 neurons per coverslip were counted. Results were derived from three to five independent experiments.

Hippocampi from mouse E16 embryonic brains were dissected in HBSS media and then partially digested with trypsin. After 15 min at 37°C, trypsin was blocked with HBSS supplemented with 10% FBS and DNase I. Cells were washed by centrifugation and resuspended in glial cell–conditioned media (neurobasal media with B27 supplement and 0.5 mM L-glutamine, which was kept overnight on glial cells) to the final density of 150,000 cells/ml. Neurons were seeded on the protein-coated coverslips (see Cell adhesion assay), and after 18-h incubation at 37°C, 5% CO_2 neurites were counted on living neurons using an inverted microscope (IMT-2; Olympus) with a 20× objective. Results were derived from three independent experiments and expressed as means ± SEM.

Cortical neuron transfilter migration assay

Cortical lobes from E15 mouse brains were dissected under a stereomicroscope and dissociated using a 20-gauge needle and a syringe in DME containing 10% FCS. The cortical preparation was spun down at 1,000 rpm for 5 min, and the pellet was washed with culture medium containing serum. The pellet was carefully resuspended, and the preparation was allowed to sediment for 5 min more before the cleared supernatant was collected. The cells in the supernatant were allowed to recover in serum-containing DME for 30–60 min. Recovered cells were washed once with the assay medium (DME with 10 mg/ml BSA, L-glutamine, and antibiotics) and resuspended in the same medium.

Transwell filters (Costar) with 12-µm pores or polycarbonate filters saturated with 100 µg/ml poly-L-lysine were coated with GDNF or ΔN-GDNF in 1-, 10-, and 100-µM concentrations overnight at 4°C and equilibrated with assay medium for 30 min in a 37°C incubator before use. The spontaneous and random migratory activity of cortical cells was controlled with uncoated filters.

Embryonic cortical cells were plated on the filters at 150,000 cells per filter and left to migrate for 16 h. Wild-type embryonic cortical cells were used to examine the migration-inducing potential of GDNF and ΔN-GDNF. Embryonic cortical cells from syndecan-3 knockout mice were used to determine the amount of migration to GDNF in the absence of syndecan-3. The filters were fixed with methanol for 20 min, stained with 1% toluidine blue for 20 min, and washed with PBS several times. After the last wash, the noncoated sides of the filters were scrubbed clean with cotton sticks, and the filters were left to dry. The number of cells that had migrated to the coated surface of the filters was calculated using an inverted light microscope (IX71; Olympus). In this assay, syndecan-3–deficient neurons and wild-type neurons migrated equally well to laminin, suggesting that the general migratory systems are intact in these knockout neurons.

Isolation of MGE cells to study GDNF-induced differentiation of GABAergic cells

MGEs were dissected from the brains of E12.5 embryos (plug day was counted as E0.5) in the HBSS buffer containing 1 mM sodium pyruvate and 10 mM Hepes, pH 7.2. MGEs were treated with 1 mg/ml papain and 10 µg/ml DNase I in HBSS containing 5 mg/ml glucose, 0.2 mg/ml BSA, and 0.5 mM EDTA at 37°C for 5–10 min. After incubation, tissues were allowed to precipitate, supernatant was replaced by trituration media (HBSS, 1 mM sodium pyruvate, 10 mM Hepes, pH 7.2, and 10 µg/ml DNase I), and trituration was performed. Trituration was repeated three times, and cell-containing supernatants were combined. Cells were precipitated by centrifugation. Cells were washed twice with growth media (neurobasal media supplemented with 100 µg/ml primocin, 2 mM glutamine, and B27 supplement), counted, and plated on poly-L-ornithine or growth factor–coated coverslips (25,000 cells per coverslip). After 48 h, cell were fixed by 4% PFA and 0.25% glutaraldehyde in PBS for 15 min.

After 48 h in culture, cells were fixed by 4% PFA and 0.25% glutaraldehyde in PBS for 15 min, washed two times with PBS, and permeabilized with PBS-T (PBS and 0.1% Triton X-100) for 15 min. Then cells were treated three times for 10 min with 1 mg/ml sodium borohydride solution and washed three times with PBS and three times with PBS-T solution. To block nonspecific binding, cells were incubated in 10% normal goat serum in PBS-T for 1 h and probed with anti-GABA antibodies (diluted 1:1,000 in blocking solution) overnight at 4°C. To visualize GABA-positive cells, anti–rabbit antibodies conjugated with Alexa Fluor 488 (diluted 1:400 in blocking solution) were used. Nuclei were stained with DAPI (Sigma-Aldrich). Unbound antibodies and DAPI were washed out with PBS-T, and coverslips were mounted in gelvatol. Epifluorescent images were collected with a microscope (BX61; Olympus) using AnalySIS acquisition software (Soft Imaging System GmbH). The length of the neurites was measured with the help of ImageJ software (National Institutes of Health).

GABAergic neuron migration assay

The final protocol was developed on the basis of the following publications: Ledda et al. (2002), Nasrallah et al. (2006), Pozas and Ibáñez (2005), Sahlberg et al. (2002), and Shulga et al. (2008). Growth factor–soaked beads were prepared as follows: 5 µl agarose beads (Affi-Gel blue; Bio-Rad Laboratories) were incubated in the PBS containing 0.1% BSA with 2 µg GDNF, ΔN-GDNF, laminin, or BDNF in the final volume of 20 µl for 1 h at 37°C. Immediately before use, beads were washed with PBS.

Brain explants were prepared as follows: brain explants containing part of the MGE and developing cortex were dissected from wild-type and syndecan-3 knockout E12.5 embryos in ice-cold Dulbecco's PBS (Life Technologies) under a stereomicroscope (MZ75; Leica). Explants were placed on 0.1-µm nucleopore polycarbonate filters positioned on top of the metal grids and cultivated on the media/air interface. Immediately after isolation, the explants were incubated in DME containing 10% FBS, GlutaMAX (Invitrogen), and primocin (InvivoGen) for 1 h, and then the media were replaced by DME containing 2× N2 supplement (Invitrogen), GlutaMAX, and primocin. Growth factor–soaked beads were placed in different positions on top of the explants under the stereomicroscope. In all experiments, beads treated with different growth factors were used for different explants produced from the same brain. Explants were cultivated in the CO_2 incubator at 37°C for 56 h and then washed once with PBS and fixed in 4% PFA overnight at 4°C.

Immunohistochemistry was performed as follows: after fixation, explants were washed in PBS, dehydrated through a graded series of methanol in PBS, and incubated in Dent's fixative (80% methanol and 20% DMSO) for 1 h. Explants were then washed in TBSTD (TBS, 0.1% Tween, and 5% DMSO) and blocked in TBSTD containing 5% BSA and 0.4% goat serum (TBSTDB) overnight at 4°C. Afterward, polyclonal rabbit anticalbindin antibodies (Swant) diluted 1:1,000 in TBSTDB were applied to the explants for 48 h at 4°C. After 2 d, explants were washed in TBSTD and incubated overnight with Alexa Fluor 488– or Alexa Fluor 568–conjugated anti–rabbit antibodies (Invitrogen) diluted 1:400 in TBSTDB. Unbound antibodies were washed off with TBSTD, and explants were mounted in gelvatol. Images were acquired with a fluorescent microscope (AX70 Provis; Olympus) using a 4× objective lens, a charge-coupled device camera, and AnalySIS acquisition software.

Densitometry was performed as follows: optical densities of selected parts of the images were measured using Aida software (Raytest). To estimate calbindin-positive neuron migration to the beads, we first calculated for each bead the difference between optical density in its close proximity and under the bead itself. This number was divided by the difference of optical densities of two circles of different diameters located approximately one bead diameter apart from the bead and normalized to their area ratio. Then, the obtained values for all beads were averaged within one explant. Results are presented as means ± SD of 7–11 independent explants from three to four litters. Statistics was performed with help of the demo version of Prism software (GraphPad Software, Inc.).

Estimation of GABAergic cell numbers in the mouse brain

The measurement of GABAergic precursor number migrating from the MGE tangentially was performed using confocal microscopy on slides stained with calbindin and Tuj1. The embryos were removed at E15 by caesarean section into the Dulbecco nutrient medium, pH 7.4, dissected out under a stereomicroscope, fixed in 4% PFA for 72 h at 4°C, cryoprotected in 30% sucrose, and cut into 50-µm-thick coronal slices with a cryostat (CM3050; Leica). Six consecutive series of slices were collected in each well, and the distance between two slices was 300 µm. The slices were collected into 15% sucrose and rinsed in PBS, pH 7.4. Slices were dehydrated in a series of methanol (30, 50, and 80% in PBS), treated in Dent's fixative, rinsed in TBSTD, pH 7.4, and then blocked in BSA-TBSTD (5% BSA and 0.4% sheep serum in TBSTD) for 3 h at room temperature. The samples were incubated in primary antibodies in BSA-TBSTD for 48 h at 4°C. The antibodies used were rabbit anticalbindin (1:400; Swant) and mouse anti-Tuj1 (1:5,000; BABCO). After washing in TBSTD, samples were placed overnight at 4°C with the specific secondary antibodies (Alexa Fluor 568 goat anti–rabbit and Alexa Fluor 488 donkey anti–mouse, 1:400; Invitrogen). The samples were rinsed in TBSTD, incubated in Hoechst (1:1,000; Invitrogen), and mounted on Superfrost Plus slides with ProLong Gold antifade reagent (Invitrogen). Z-series image stacks were acquired with a confocal microscope (TCS SP5; Leica) using an HCX Plan Apochromat 20× glycerol objective and analyzed with the software Imaris (Bitplane). Calbindin-positive cells were counted with the experimenter blind to the genotype of the sample from the medial area of embryonic brain at the medial and the lateral part of the cortical plate and the IZ of the GEs. The intensity of Tuj1 epifluorescence was measured with Image-Pro software (Media Cybernetics). The Student's *t* tests were performed using Excel 2007 software (Microsoft).

To count GABAergic neurons in the adult cortex, 5-mm-thick coronal paraffin sections from adult syndecan-3 wild-type and knockout brains were dewaxed and hydrated. 1 µg/ml antibodies against GABA (Millipore) was diluted in PBS containing 2% BSA and 0.3% Triton X-100. The sections were incubated with the antibody solution overnight, and biotinylated secondary antibodies were used to detect the immunostaining signal. For quantifications, the required brain areas (dorsomedial, dorsolateral, and lateral cortices) were photographed at 63× magnification with a camera (AxioCam; Carl Zeiss, Inc.) mounted in a microscope (AxioPlan; Carl Zeiss, Inc.). Cell density estimates from photographs were made by the selector method (Everall et al., 1997) using ImageJ software.

Online supplemental material

Fig. S1 shows GFL interaction with desulfated heparins. Fig. S2 shows the characterization of the ΔN-GDNF variant and SHEP cell spreading. Fig. S3 shows differentiation of GABAergic cells in the culture of E12.5 MGE cells on immobilized GDNF. Fig. S4 shows the migration assay of GABAergic neurons. Video 1 shows live imaging of SHEP cells spreading on immobilized GDNF. Table S1 shows the analysis of GFL binding to heparin and syndecan-3. Online supplemental material is available at http://www.jcb.org/cgi/content/full/jcb.201009136/DC1.

We are thankful to Dr. David Kaplan, Dr. Ryo Takano, and Dr. Ulf Lindahl for reagents. We thank Amgen, Inc. for G90 antibodies. Satu Åkerberg, Svetlana Vasilieva, Miika Palviainen, Riikka Santalahti, and Dr. Pia Runeberg-Roos are thanked for the help in experiments. We are grateful to Dr. Urmas Arumäe, Dr. Veli-Matti Leppänen, Dr. Pia Runeberg-Roos, Dr. Matti S. Airaksinen, Dr. Matthew Philips, Dr. Edgar R. Kramer, Prof. Adrian Goldman, Prof. Hannu Sariola, and Prof. Klaus Unsiker for useful comments and criticism. We wish to thank Jan Mattila, Timo "Tinde" Päivärinta, and Dr. Matti S. Airaksinen for the help with the graphic art.

This work was supported by the Institute of Biotechnology, Neuroscience Center, Academy of Finland program 11186236 (Finnish Centre of Excellence Program 2008–2013), European Union grant QLG3-CT-2002-01000, and Sigrid Jusélius Foundation grants to H. Rauvala and M. Saarma. M.M. Bespalov was supported by the Centre for International Mobility and the Graduate School for Biotechnology and Molecular Biology from 2001 to 2006. S. Tumova was supported by a postdoctoral fellowship from the Academy of Finland from 2002 to 2004.

Submitted: 30 September 2010
Accepted: 3 December 2010

References

Alfano, I., P. Vora, R.S. Mummery, B. Mulloy, and C.C. Rider. 2007. The major determinant of the heparin binding of glial cell-line-derived neurotrophic factor is near the N-terminus and is dispensable for receptor binding. *Biochem. J.* 404:131–140. doi:10.1042/BJ20061747

Barnett, M.W., C.E. Fisher, G. Perona-Wright, and J.A. Davies. 2002. Signalling by glial cell line-derived neurotrophic factor (GDNF) requires heparan sulphate glycosaminoglycan. *J. Cell Sci.* 115:4495–4503. doi:10.1242/jcs.00114

Bernfield, M., M. Götte, P.W. Park, O. Reizes, M.L. Fitzgerald, J. Lincecum, and M. Zako. 1999. Functions of cell surface heparan sulfate proteoglycans. *Annu. Rev. Biochem.* 68:729–777. doi:10.1146/annurev.biochem.68.1.729

Bespalov, M.M., and M. Saarma. 2007. GDNF family receptor complexes are emerging drug targets. *Trends Pharmacol. Sci.* 28:68–74. doi:10.1016/j.tips.2006.12.005

Bishop, J.R., M. Schuksz, and J.D. Esko. 2007. Heparan sulphate proteoglycans fine-tune mammalian physiology. *Nature.* 446:1030–1037. doi:10.1038/nature05817

Bullock, S.L., J.M. Fletcher, R.S. Beddington, and V.A. Wilson. 1998. Renal agenesis in mice homozygous for a gene trap mutation in the gene encoding heparan sulfate 2-sulfotransferase. *Genes Dev.* 12:1894–1906. doi:10.1101/gad.12.12.1894

Cardin, A.D., and H.J. Weintraub. 1989. Molecular modeling of protein-glycosaminoglycan interactions. *Arteriosclerosis.* 9:21–32.

Cik, M., S. Masure, A.S. Lesage, I. Van Der Linden, P. Van Gompel, M.N. Pangalos, R.D. Gordon, and J.E. Leysen. 2000. Binding of GDNF and neurturin to human GDNF family receptor alpha 1 and 2. Influence of cRET and cooperative interactions. *J. Biol. Chem.* 275:27505–27512.

Eketjäll, S., M. Fainzilber, J. Murray-Rust, and C.F. Ibáñez. 1999. Distinct structural elements in GDNF mediate binding to GFRalpha1 and activation of the GFRalpha1-c-Ret receptor complex. *EMBO J.* 18:5901–5910. doi:10.1093/emboj/18.21.5901

Everall, I.P., R. DeTeresa, R. Terry, and E. Masliah. 1997. Comparison of two quantitative methods for the evaluation of neuronal number in the frontal cortex in Alzheimer disease. *J. Neuropathol. Exp. Neurol.* 56:1202–1206. doi:10.1097/00005072-199711000-00004

Geiger, B., A. Bershadsky, R. Pankov, and K.M. Yamada. 2001. Transmembrane crosstalk between the extracellular matrix—cytoskeleton crosstalk. *Nat. Rev. Mol. Cell Biol.* 2:793–805. doi:10.1038/35099066

Gill, S.S., N.K. Patel, G.R. Hotton, K. O'Sullivan, R. McCarter, M. Bunnage, D.J. Brooks, C.N. Svendsen, and P. Heywood. 2003. Direct brain infusion of glial cell line-derived neurotrophic factor in Parkinson disease. *Nat. Med.* 9:589–595. doi:10.1038/nm850

Golden, J.P., J.A. DeMaro, P.A. Osborne, J. Milbrandt, and E.M. Johnson Jr. 1999. Expression of neurturin, GDNF, and GDNF family-receptor mRNA in the developing and mature mouse. *Exp. Neurol.* 158:504–528. doi:10.1006/exnr.1999.7127

Hamilton, J.F., P.F. Morrison, M.Y. Chen, J. Harvey-White, R.S. Pernaute, H. Phillips, E. Oldfield, and K.S. Bankiewicz. 2001. Heparin coinfusion during convection-enhanced delivery (CED) increases the distribution of the glial-derived neurotrophic factor (GDNF) ligand family in rat striatum and enhances the pharmacological activity of neurturin. *Exp. Neurol.* 168:155–161. doi:10.1006/exnr.2000.7571

Henderson, C.E., H.S. Phillips, R.A. Pollock, A.M. Davies, C. Lemeulle, M. Armanini, L. Simmons, B. Moffet, R.A. Vandlen, L. Simmons, et al. 1994. GDNF: a potent survival factor for motoneurons present in peripheral nerve and muscle. *Science.* 266:1062–1064. doi:10.1126/science.7973664

Hienola, A., S. Tumova, E. Kulesskiy, and H. Rauvala. 2006. N-syndecan deficiency impairs neural migration in brain. *J. Cell Biol.* 174:569–580. doi:10.1083/jcb.200602043

Hileman, R.E., J.R. Fromm, J.M. Weiler, and R.J. Linhardt. 1998. Glycosaminoglycan-protein interactions: definition of consensus sites in glycosaminoglycan binding proteins. *Bioessays.* 20:156–167. doi:10.1002/(SICI)1521-1878(199802)20:2<156::AID-BIES8>3.0.CO;2-R

Hynes, R.O. 1999. Cell adhesion: old and new questions. *Trends Cell Biol.* 9:M33–M37. doi:10.1016/S0962-8924(99)01667-0

Ikeda, T., X.Y. Xia, Y.X. Xia, T. Ikenoue, and B.H. Choi. 1999. Expression of glial cell line-derived neurotrophic factor in the brain and cerebrospinal fluid of the developing rat. *Int. J. Dev. Neurosci.* 17:681–691. doi:10.1016/S0736-5748(99)00057-X

Inatani, M., F. Irie, A.S. Plump, M. Tessier-Lavigne, and Y. Yamaguchi. 2003. Mammalian brain morphogenesis and midline axon guidance require heparan sulfate. *Science.* 302:1044–1046. doi:10.1126/science.1090497

Keinänen, K., A. Jouppila, and A. Kuusinen. 1998. Characterization of the kainate-binding domain of the glutamate receptor GluR-6 subunit. *Biochem. J.* 330:1461–1467.

Kinnunen, A., M. Niemi, T. Kinnunen, M. Kaksonen, R. Nolo, and H. Rauvala. 1999. Heparan sulphate and HB-GAM (heparin-binding growth-associated molecule) in the development of the thalamocortical pathway of rat brain. *Eur. J. Neurosci.* 11:491–502. doi:10.1046/j.1460-9568.1999.00457.x

Kinnunen, T., M. Kaksonen, J. Saarinen, N. Kalkkinen, H.B. Peng, and H. Rauvala. 1998. Cortactin-Src kinase signaling pathway is involved in N-syndecan-dependent neurite outgrowth. *J. Biol. Chem.* 273:10702–10708. doi:10.1074/jbc.273.17.10702

Koo, H., and B.H. Choi. 2001. Expression of glial cell line-derived neurotrophic factor (GDNF) in the developing human fetal brain. *Int. J. Dev. Neurosci.* 19:549–558. doi:10.1016/S0736-5748(01)00042-9

Lang, A.E., S. Gill, N.K. Patel, A. Lozano, J.G. Nutt, R. Penn, D.J. Brooks, G. Hotton, E. Moro, P. Heywood, et al. 2006. Randomized controlled trial of intraputamenal glial cell line-derived neurotrophic factor infusion in Parkinson disease. *Ann. Neurol.* 59:459–466. doi:10.1002/ana.20737

Lauri, S.E., S. Kaukinen, T. Kinnunen, A. Ylinen, S. Imai, K. Kaila, T. Taira, and H. Rauvala. 1999. Reg1ulatory role and molecular interactions of a cell-surface heparan sulfate proteoglycan (N-syndecan) in hippocampal long-term potentiation. *J. Neurosci.* 19:1226–1235.

Ledda, F., G. Paratcha, and C.F. Ibáñez. 2002. Target-derived GFRalpha1 as an attractive guidance signal for developing sensory and sympathetic axons via activation of Cdk5. *Neuron.* 36:387–401. doi:10.1016/S0896-6273(02)01002-4

Ledda, F., G. Paratcha, T. Sandoval-Guzmán, and C.F. Ibáñez. 2007. GDNF and GFRalpha1 promote formation of neuronal synapses by ligand-induced cell adhesion. *Nat. Neurosci.* 10:293–300. doi:10.1038/nn1855

Leppänen, V.M., M.M. Bespalov, P. Runeberg-Roos, U. Puurand, A. Merits, M. Saarma, and A. Goldman. 2004. The structure of GFRalpha1 domain 3 reveals new insights into GDNF binding and RET activation. *EMBO J.* 23:1452–1462. doi:10.1038/sj.emboj.7600174

Li, J.P., F. Gong, A. Hagner-McWhirter, E. Forsberg, M. Abrink, R. Kisilevsky, X. Zhang, and U. Lindahl. 2003. Targeted disruption of a murine glucuronyl C5-epimerase gene results in heparan sulfate lacking L-iduronic acid and in neonatal lethality. *J. Biol. Chem.* 278:28363–28366. doi:10.1074/jbc.C300219200

Lin, L.F., D.H. Doherty, J.D. Lile, S. Bektesh, and F. Collins. 1993. GDNF: a glial cell line-derived neurotrophic factor for midbrain dopaminergic neurons. *Science.* 260:1130–1132. doi:10.1126/science.8493557

Lindahl, M., T. Timmusk, J. Rossi, M. Saarma, and M.S. Airaksinen. 2000. Expression and alternative splicing of mouse Gfra4 suggest roles in endocrine cell development. *Mol. Cell. Neurosci.* 15:522–533. doi:10.1006/mcne.2000.0845

Lindahl, M., D. Poteryaev, L. Yu, U. Arumäe, T. Timmusk, I. Bongarzone, A. Aiello, M.A. Pierotti, M.S. Airaksinen, and M. Saarma. 2001. Human glial cell line-derived neurotrophic factor receptor alpha 4 is the receptor for persephin and is predominantly expressed in normal and malignant thyroid medullary cells. *J. Biol. Chem.* 276:9344–9351. doi:10.1074/jbc.M008279200

Marín, O., and J.L. Rubenstein. 2003. Cell migration in the forebrain. *Annu. Rev. Neurosci.* 26:441–483. doi:10.1146/annurev.neuro.26.041002.131058

Moore, M.W., R.D. Klein, I. Fariñas, H. Sauer, M. Armanini, H. Phillips, L.F. Reichardt, A.M. Ryan, K. Carver-Moore, and A. Rosenthal. 1996. Renal and neuronal abnormalities in mice lacking GDNF. *Nature.* 382:76–79. doi:10.1038/382076a0

Nasrallah, I.M., M.F. McManus, M.M. Pancoast, A. Wynshaw-Boris, and J.A. Golden. 2006. Analysis of non-radial interneuron migration dynamics

and its disruption in Lis1+/- mice. *J. Comp. Neurol.* 496:847–858. doi:10.1002/cne.20966

Nolo, R., M. Kaksonen, E. Raulo, and H. Rauvala. 1995. Co-expression of heparin-binding growth-associated molecule (HB-GAM) and N-syndecan (syndecan-3) in developing rat brain. *Neurosci. Lett.* 191:39–42. doi:10.1016/0304-3940(94)11551-1

Paratcha, G., F. Ledda, and C.F. Ibáñez. 2003. The neural cell adhesion molecule NCAM is an alternative signaling receptor for GDNF family ligands. *Cell.* 113:867–879. doi:10.1016/S0092-8674(03)00435-5

Parkash, V., V.M. Leppänen, H. Virtanen, J.M. Jurvansuu, M.M. Bespalov, Y.A. Sidorova, P. Runeberg-Roos, M. Saarma, and A. Goldman. 2008. The structure of the glial cell line-derived neurotrophic factor-coreceptor complex: insights into RET signalling and heparin binding. *J. Biol. Chem.* 283:35164–35172.

Paveliev, M., M.S. Airaksinen, and M. Saarma. 2004. GDNF family ligands activate multiple events during axonal growth in mature sensory neurons. *Mol. Cell. Neurosci.* 25:453–459. doi:10.1016/j.mcn.2003.11.010

Pichel, J.G., L. Shen, H.Z. Sheng, A.C. Granholm, J. Drago, A. Grinberg, E.J. Lee, S.P. Huang, M. Saarma, B.J. Hoffer, et al. 1996. Defects in enteric innervation and kidney development in mice lacking GDNF. *Nature.* 382:73–76. doi:10.1038/382073a0

Piltonen, M., M.M. Bespalov, D. Ervasti, T. Matilainen, Y.A. Sidorova, H. Rauvala, M. Saarma, and P.T. Männistö. 2009. Heparin-binding determinants of GDNF reduce its tissue distribution but are beneficial for the protection of nigral dopaminergic neurons. *Exp. Neurol.* 219:499–506. doi:10.1016/j.expneurol.2009.07.002

Poteryaev, D., A. Titievsky, Y.F. Sun, J. Thomas-Crusells, M. Lindahl, M. Billaud, U. Arumäe, and M. Saarma. 1999. GDNF triggers a novel ret-independent Src kinase family-coupled signaling via a GPI-linked GDNF receptor alpha1. *FEBS Lett.* 463:63–66. doi:10.1016/S0014-5793(99)01590-2

Pozas, E., and C.F. Ibáñez. 2005. GDNF and GFRalpha1 promote differentiation and tangential migration of cortical GABAergic neurons. *Neuron.* 45:701–713. doi:10.1016/j.neuron.2005.01.043

Raulo, E., M.A. Chernousov, D.J. Carey, R. Nolo, and H. Rauvala. 1994. Isolation of a neuronal cell surface receptor of heparin binding growth-associated molecule (HB-GAM). Identification as N-syndecan (syndecan-3). *J. Biol. Chem.* 269:12999–13004.

Rauvala, H. 1989. An 18-kd heparin-binding protein of developing brain that is distinct from fibroblast growth factors. *EMBO J.* 8:2933–2941.

Rauvala, H., H.J. Huttunen, C. Fages, M. Kaksonen, T. Kinnunen, S. Imai, E. Raulo, and I. Kilpeläinen. 2000. Heparin-binding proteins HB-GAM (pleiotrophin) and amphoterin in the regulation of cell motility. *Matrix Biol.* 19:377–387. doi:10.1016/S0945-053X(00)00084-6

Reizes, O., J. Lincecum, Z. Wang, O. Goldberger, L. Huang, M. Kaksonen, R. Ahima, M.T. Hinkes, G.S. Barsh, H. Rauvala, and M. Bernfield. 2001. Transgenic expression of syndecan-1 uncovers a physiological control of feeding behavior by syndecan-3. *Cell.* 106:105–116. doi:10.1016/S0092-8674(01)00415-9

Rickard, S.M., R.S. Mummery, B. Mulloy, and C.C. Rider. 2003. The binding of human glial cell line-derived neurotrophic factor to heparin and heparan sulfate: importance of 2-O-sulfate groups and effect on its interaction with its receptor, GFRalpha1. *Glycobiology.* 13:419–426. doi:10.1093/glycob/cwg046

Rider, C.C. 2003. Interaction between glial-cell-line-derived neurotrophic factor (GDNF) and 2-O-sulphated heparin-related glycosaminoglycans. *Biochem. Soc. Trans.* 31:337–339. doi:10.1042/BST0310337

Sahlberg, C., T. Mustonen, and I. Thesleff. 2002. Explant cultures of embryonic epithelium. Analysis of mesenchymal signals. *Methods Mol. Biol.* 188:373–382.

Sariola, H., and M. Saarma. 2003. Novel functions and signalling pathways for GDNF. *J. Cell Sci.* 116:3855–3862. doi:10.1242/jcs.00786

Shulga, A., J. Thomas-Crusells, T. Sigl, A. Blaesse, P. Mestres, M. Meyer, Q. Yan, K. Kaila, M. Saarma, C. Rivera, and K.M. Giehl. 2008. Posttraumatic GABA(A)-mediated [Ca2+]i increase is essential for the induction of brain-derived neurotrophic factor-dependent survival of mature central neurons. *J. Neurosci.* 28:6996–7005. doi:10.1523/JNEUROSCI.5268-07.2008

Silvian, L., P. Jin, P. Carmillo, P.A. Boriack-Sjodin, C. Pelletier, M. Rushe, B. Gong, D. Sah, B. Pepinsky, and A. Rossomando. 2006. Artemin crystal structure reveals insights into heparan sulfate binding. *Biochemistry.* 45:6801–6812. doi:10.1021/bi060035x

Slevin, J.T., G.A. Gerhardt, C.D. Smith, D.M. Gash, R. Kryscio, and B. Young. 2005. Improvement of bilateral motor functions in patients with Parkinson disease through the unilateral intraputaminal infusion of glial cell line-derived neurotrophic factor. *J. Neurosurg.* 102:216–222. doi:10.3171/jns.2005.102.2.0216

Takano, R., Z. Ye, T.V. Ta, K. Hayashi, H. Kato, Y. Kariya, and S. Hara. 1998. Specific 6-O-desulfation of heparin. *Carbohydr. Lett.* 3:71–77.

Trupp, M., N. Belluardo, H. Funakoshi, and C.F. Ibáñez. 1997. Complementary and overlapping expression of glial cell line-derived neurotrophic factor (GDNF), c-ret proto-oncogene, and GDNF receptor-alpha indicates multiple mechanisms of trophic actions in the adult rat CNS. *J. Neurosci.* 17:3554–3567.

Van Vactor, D., D.P. Wall, and K.G. Johnson. 2006. Heparan sulfate proteoglycans and the emergence of neuronal connectivity. *Curr. Opin. Neurobiol.* 16:40–51. doi:10.1016/j.conb.2006.01.011

Weinacker, A., A. Chen, M. Agrez, R.I. Cone, S. Nishimura, E. Wayner, R. Pytela, and D. Sheppard. 1994. Role of the integrin alpha v beta 6 in cell attachment to fibronectin. Heterologous expression of intact and secreted forms of the receptor. *J. Biol. Chem.* 269:6940–6948.

Xu, R.Y., K. Pong, Y. Yu, D. Chang, S. Liu, J.D. Lile, J. Treanor, K.D. Beck, and J.C. Louis. 1998. Characterization of two distinct monoclonal antibodies specific for glial cell line-derived neurotrophic factor. *J. Neurochem.* 70:1383–1393. doi:10.1046/j.1471-4159.1998.70041383.x

Ylikoski, J., U. Pirvola, M. Moshnyakov, J. Palgi, U. Arumäe, and M. Saarma. 1993. Expression patterns of neurotrophin and their receptor mRNAs in the rat inner ear. *Hear. Res.* 65:69–78. doi:10.1016/0378-5955(93)90202-C

Yoneda, A., and J.R. Couchman. 2003. Regulation of cytoskeletal organization by syndecan transmembrane proteoglycans. *Matrix Biol.* 22:25–33. doi:10.1016/S0945-053X(03)00010-6